



KTH Electrical Engineering

Plasma-facing components in tokamaks: material modification and fuel retention

DARYA IVANOVA

Doctoral Thesis
Stockholm, Sweden 2012

TRITA-EE 2012:058
ISSN 1653-5146
ISBN 978-91-7501-567-5

KTH School of Electrical Engineering (EES)
SE-100 44 Stockholm
Sweden

Akademisk avhandling som med tillstånd av Kungl Tekniska högskolan framlägges till offentlig granskning för avläggande av Technologie doktorsexamen i fysikalisk elektroteknik onsdagen den 12 december 2012 klockan 10.00 i Sal F3, Lindstedtsvägen 26, Kungliga Tekniska högskolan, Stockholm.

© Darya Ivanova, November 5, 2012 (document build date)

Tryck: Universitetsservice US AB

Abstract

Fuel inventory and generation of carbon and metal dust in a tokamak are perceived to be serious safety and economy issues for the steady-state operation of a fusion reactor, e.g. ITER. These topics have been explored in this thesis in order to contribute to a better understanding and the development of methods for controlling and curtailing fuel accumulation and dust formation in controlled fusion devices. The work was carried out with material facing fusion plasmas in three tokamaks: TEXTOR in Forschungszentrum Jülich (Germany), Tore Supra in the Nuclear Research Center Cadarache (France) and JET in Culham Centre for Fusion Energy (United Kingdom). Following issues were addressed: (a) properties of material migration products, i.e. co-deposited layers and dust particles; (b) impact of fuel removal methods on dust generation and on modification of plasma-facing components; (c) efficiency of fuel and deposit removal techniques; (d) degradation mechanism of diagnostic components - mirrors - and methods of their regeneration. The study dealt with carbon, tungsten and beryllium, i.e. with the three major elements used as wall materials in present-day devices and foreseen for a next-step machine.

List of Papers

This thesis is based on the work presented in the following papers:

- I *Survey of dust formed in the TEXTOR tokamak: structure and fuel retention.*
D. Ivanova, M. Rubel, V. Philipps, M. Freisinger, Z. Huang, H. Penkalla, B. Schweer, G. Sergienko, P. Sundelin, E. Wessel
Physica Scripta T138 (2009) 014025.
- II *Laser-based and thermal methods for fuel removal and cleaning of plasma-facing components.*
D. Ivanova, M. Rubel, V. Philipps, B. Schweer, M. Freisinger, A. Huber, N. Gierse, H. Penkalla, P. Petersson, T. Dittmar
Journal of Nuclear Materials, 415 (2011) S801-S804.
- III *Fuel re-absorption by thermally treated co-deposited carbon layers.*
D. Ivanova, M. Rubel, V. Philipps, B. Schweer, P. Petersson, M. Freisinger, A. Schmidt
Physica Scripta T145 (2011) 014006.
- IV *Efficiency of fuel removal techniques tested on plasma-facing components from the TEXTOR tokamak.*
M. Rubel, **D. Ivanova**, V. Philipps, M. Zlobinski, A. Huber, P. Petersson, B. Schweer
Fusion Engineering and Design, 87 (2012) 935-940.
- V *Comparison of JET main chamber erosion with dust collected in the divertor.*
A. Widdowson, C.F. Ayres, S. Booth, J. P. Coad, A. Hakola, **D. Ivanova**, S. Koivuranta, J. Likonen, M. Mayer, M. Stamp
Journal of Nuclear Materials, *submitted*.

VI *Removal of beryllium-containing films deposited in JET from mirror surfaces by laser cleaning.*

A. Widdowson, J.P. Coad, G. de Temmerman, D. Farcage, D. Hole, **D. Ivanova**, A. Leontyev, M. Rubel, A. Semerok, A. Schmidt, P.-Y. Thro
Journal of Nuclear Materials, 415 (2011) S1199-S1202.

VII *Overview of the second stage in the comprehensive mirrors test in JET.*

M. Rubel, **D. Ivanova**, J. P. Coad, G. De Temmerman, J. Likonen, L. Marot, A. Schmidt, A. Widdowson
Physica Scripta T145 (2011) 014070.

VIII *Assessment of cleaning methods for first mirrors tested in JET for ITER.*

D. Ivanova, A. Widdowson, J. Likonen, L. Marot, S. Koivuranta, J.P. Coad, M. Rubel, P. Petterson, G. De Temmerman
Journal of Nuclear Materials, *submitted*.

My contributions:

This section comprises a statement on my involvement and role in the papers included in the thesis. In four cases (*Papers I, II, III, VIII*) I was fully responsible for their content and structure. In other cases I was responsible for part of the studies: measurements, data analysis of certain section. In all cases I took part in the formulation of statements in the discussion of results and the final version of the papers.

Paper I I assessed the properties of the deposited layers, participated in the thermal desorption and ion beam studies, performed the full data analysis i.e. the determination of fuel content, wrote the paper and presented the results at the PFMC-12 workshop, Jülich, Germany, May 2009 (poster).

Papers II and III I was involved in every step of the planning and performing of the experiments and measurements, in the analysis of the obtained data and the discussion of the results. I wrote the papers and presented the results at the PSI-19 conference, San Diego, USA, May 2010 (Paper II, poster) and at the PFMC-13 conference, Rosenheim, Germany, May 2011 (Paper III, poster).

Paper IV I participated in the experiments (laser-based and thermal fuel removal techniques), analysis of results and in writing the paper. I also presented the poster at the ISFNT-10 conference, Portland, USA, September 2011.

Paper V I was responsible for the estimation of the carbon erosion yield from the main wall of JET operated with a carbon wall (last operation period) in order to compare the erosion with the amount of carbon dust retrieved during the JET shut-down for the ITER-like wall installation. My work comprised:

- analysis of spectroscopy data for over 10000 discharges;
- assessment of the eroded amount of carbon;
- interpretation of results and participation in discussions.

Paper VI I was directly involved in the assessment of the surface state of the metallic mirrors and cassettes before and after the laser-induced cleaning. The assessment was based on the spectrophotometry and ion beam analysis.

Paper VII I was involved in the studies of the performance of mirrors after exposure in JET, participated in writing the paper and presented the results at the PFMC-13 conference, Rosenheim, Germany, May 2011 (talk). There were the following components of my involvement:

- measurements of mirror reflectivity after exposure in JET;
- participation in ion beam analysis of surface composition of mirrors after exposure (a different set of mirrors from that in Paper VI);
- analysis of data from the SIMS and EDX measurements;
- interpretation of results.

Paper VIII I was responsible for the work and I was involved in all steps reported in the paper: planning work, experiments, measurements, data analysis, interpretation and discussion. I studied the state of the mirror surfaces before and after the cleaning based on the measurements performed by me (reflectivity, ion beam analysis) and my colleagues. I wrote the paper and presented the results at the PSI-20 conference, Aachen, Germany, May 2012 (poster).

Acknowledgements

Many people contributed to this thesis in countless ways, and I am grateful to all of them.

First of all, I thank my supervisor Marek Rubel for his patience and advice, for always being around to help and to share his knowledge. Special gratitude also goes to my second supervisor Per Brunzell and to James Drake for being ready to answer all my questions.

My research required a lot of travelling and a large part of the work was done outside Sweden, namely in Forschungszentrum Jülich (Germany) and Culham Center for Fusion Energy (United Kingdom). I am grateful to all the people at these research centers who not only provided me with access to laboratory equipment and assisted me during measurements but also helped with valuable discussions of the results. In particular, I would like to thank Volker Phillips, Sebastian Brezinsek, Bernd Schweer, Alexander Huber, Arkadi Kreter, Gennadi Sergienko, Anna Widdowson and Paul Coad for coordinating my work. It was a great pleasure to work with you.

Not all trips were that distant. Numerous measurements were performed at the Ångström Laboratory of Uppsala University and that would not have been possible without Per Petersson and Jonas Åström whose help during the ion beam analysis was invaluable. I also thank Göran Possnert for all arrangements.

When one designs new experiments, not much can be done without the help of good engineers. Håkan, Jesper and Lars - thank you for being prompt with manufacturing all the holders, probes and other strange details without complicated and precise drawings. Michael - thank you for all your help with the thermal desorption measurements.

In addition, I would like to thank all the people whose support made it easier to understand all the paperwork associated with doctoral studies as well as to arrange my visits to Jülich and Culham. Bojan, Jeanette and Emma in Alfvén Lab and Angelika in FZ Jülich were always offering fast and efficient solutions when it came to administrative matters.

Furthermore, there were other PhD students, postdocs, and just friends who provided a very pleasant and cheerful atmosphere during my stay in Sweden and abroad: Jan, Dmitry, Maria, Lorenzo, Igor and Per. You all know how emotional and stressed I can be sometimes, so your support was priceless.

Finally, I thank my family and friends back home in Russia for their understanding and continuous support. And, of course, Koen.

Thank you all! If I forgot to mention anyone, it is not intentional.

Abbreviations

ALT II	Advanced Limiter Test II (TEXTOR)
BEI	Backscattering Electron Image
CFC	Carbon Fibre Composite
DED	Dynamic Ergodic Divertor (TEXTOR)
DEMO	DEMOstration power plant
DITS	Deuterium in Tore Supra (project)
EDX(EDS)	Energy Dispersive X-ray Analysis
EFDA	European Fusion Development Agreement
ELM	Edge Localised Mode
EPS	Enhanced Proton Scattering
ERDA	Elastic Recoil Detection Analysis
FMT	First Mirror Test
IBA	Ion Beam Analysis
ICF	Inertial Confinement Fusion
ICWC	Ion Cyclotron Wall Conditioning
ILW	ITER-Like Wall (JET)
IR	Infrared (light)
ITER	International Thermonuclear Experimental Reactor
JET	Joint European Torus
MCF	Magnetic Confinement Fusion
NRA	Nuclear Reaction Analysis
PFC	Plasma-Facing Component(s)
PFM	Plasma-Facing Material(s)
PSI	Plasma-Surface Interactions
PWI	Plasma-Wall Interactions
QMS	Quadrupole Mass Spectrometer
RBS	Rutherford Backscattering Spectroscopy
RF	Radio Frequency
SEI	Secondary Electron Image
SEM	Scanning Electron Microscopy
SIMS	Secondary Ion Mass Spectrometry

TDS	Thermal Desorption Spectrometry
TEM	Transmission Electron Microscopy
TEXTOR	Toroidal Experiment for Technology Oriented Research
ToF	Time-of-Flight
TPL	Toroidal Pump Limiter (Tore Supra)
VPS	Vacuum Plasma Sprayed (coatings)
WDS	Wavelength Dispersive X-ray Spectroscopy

Contents

List of Papers	v
Acknowledgements	ix
Abbreviations	xi
Contents	xiii
1 Introduction	1
1.1 Fusion reactions	2
1.2 Fusion devices	4
2 Plasma-wall interactions	11
2.1 Plasma-facing materials for ITER	12
2.2 Material migration: erosion-deposition processes	14
2.3 Dust in fusion devices	17
2.4 Fuel inventory	20
3 Removal of fuel and co-deposits	23
3.1 Thermal methods	23
3.2 Photonic methods	24
3.3 Plasma-assisted methods	25
3.4 Ion cyclotron wall conditioning	25
3.5 Mechanical cleaning	26
4 Surface morphology studies	29
4.1 Electron microscopy	29
4.2 Surface profilometry	31
4.3 Ion beam analysis	32
4.4 Gas phase control	37
5 Impact of PWI on diagnostic components	39
5.1 Diagnostic mirrors	39

5.2 First Mirror Test at JET	39
6 Summary	43
References	47

Chapter 1

Introduction

In the matter of physics, the first lessons should contain nothing but what is experimental and interesting to see.

Albert Einstein

The sustainable development of our civilisation is strongly dependent on the energy supply. This means both the access to resources and the exploitation of efficient energy production and saving methods. There is also a great need for doing it in a way least harmful for the environment, i.e. reduced contamination and CO₂ release. Over the last 40 years the electricity production in developed countries has been based on coal, gas, oil, water and nuclear fission. The role of renewable sources, e.g. solar irradiation, wind and biomass, remains minor despite huge investments and technology improvements [1][2]. The progress in nuclear industry is also of great importance as this supplier of electricity would reduce the problem of the emission of greenhouse gases, yet nuclear fission has the drawback of producing long-term contaminated waste. Nuclear fusion is considered to be an attractive solution for the future global energy mix. The aim of fusion research is to construct and operate a power-generating plant by harnessing on Earth reactions occurring in stars.

The Sun has always been associated in human minds with a source of energy. The physical working principles of this natural reactor were suggested by Hans Bethe in 1939 [3], which brought him the Nobel Prize in 1967. The idea of a huge energy release as a result of merging lighter nuclei was very appealing for military purpose and the thermonuclear weapon research was started immediately. In the early 1950's research in the direction of controlled magnetic fusion as an energy source began simultaneously in the USA, the United Kingdom and the Soviet Union. Since the first international fusion conference in 1958 these countries have been working in collaboration with each other. Throughout the following decades many other countries joined fusion research. A major achievement of this multi-national community is the agreement to build the International Thermonuclear

Experimental Reactor (ITER), which is already under construction in the south of France (Cadarache) [4]. ITER will be the first fusion experiment to demonstrate a positive energy output. It will also provide the knowledge necessary for the design of the next-step device: a reactor for a demonstration fusion power plant (DEMO).

1.1 Fusion reactions

“*Nuclear fusion*” denotes a fusion reaction of two light nuclei with products in the form of a heavier nucleus and an energy release. Each nuclear reaction is unique and is characterised by an energy yield Q and an energy-dependent cross-section σ , i.e. a measure for the probability that the Coulomb barrier is overcome and nuclear reaction can occur. The reaction rate of a nuclear reaction denotes the number of reactions per unit volume per unit time and is proportional to $\langle \sigma v \rangle$, which is an average of the product of the cross-section (σ) and the relative velocity (v) of the nuclei over the velocity distribution. A candidate reaction for a commercial power plant must satisfy two main criteria: the reaction must be exothermic ($Q > 0$) and the cross-section must be high enough at achievable energies. In order to achieve controlled thermonuclear fusion under terrestrial conditions the efforts are concentrated on reactions between light nuclei, especially hydrogen isotopes. Some of the considered reactions with the corresponding Q - values are listed below and their reaction rates for are shown in Figure 1.1. The branching ratio of two D-D reactions (b_1) and (b_2) is about 50% so the sum of the reaction rates is included in the figure:

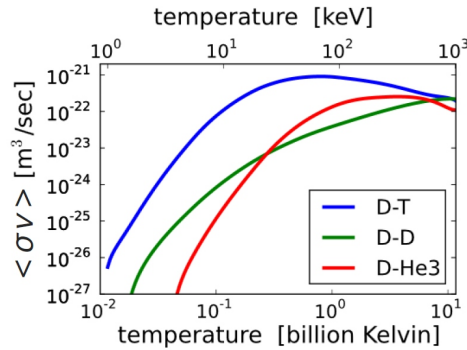
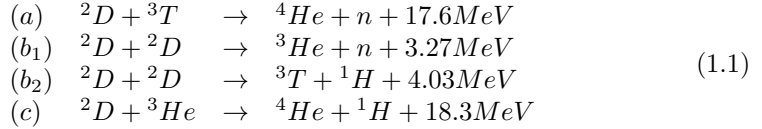
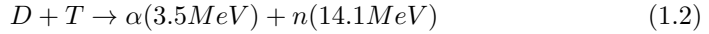


Figure 1.1: Reaction rates of the D-T, D-D and D- ${}^3\text{He}$ reactions.

The D-T reaction is the most favourable due to a higher cross section at energies, achievable at the present level of technology [5]. Furthermore, the D-T reaction has a relatively small variation in cross-section at the energy of interest (10 – 30 keV). As a consequence of the conservation of mass and energy, the energy in the reactions with two products is divided between them in inverse proportion to their masses. Taking this into account and using another common notation for energetic ${}^4\text{He}$ ions (α -particles), the D-T reaction (Eq. 1.1a) can be rewritten as:



The positively charged α -particles from the D-T fusion remain confined and deliver their energy to the background plasma, and are thus essential for plasma heating and partly compensate for the energy losses. Energetic neutrons escape the plasma volume. In the *blanket* their kinetic energy is to be converted into heat and then into electricity in a similar manner as in conventional nuclear or fossil fuel thermal power plants.

A major requirement for fusion as a commercial source of energy is *fuel self-sufficiency* [6]. Deuterium and tritium are both isotopes of hydrogen but their natural abundance differs strongly. While deuterium is easy to obtain from water (natural abundance 0.015%), tritium must be produced, as there is no available natural source of tritium on Earth because of a short tritium half-life (12.32 years). In a fusion reactor *breeding* of tritium will be achieved by bombarding lithium¹ isotopes with neutrons [5]. Since neutrons are already present as a product of the D-T reaction, tritium breeding modules can be installed directly in the protecting blanket of a fusion reactor and several such modules will be tested already in ITER [7]. The resulting fuel cycle in a fusion reactor with the impact of tritium breeding is schematically shown in Figure 1.2. The most required is the reaction of neutrons with ${}^6\text{Li}$.

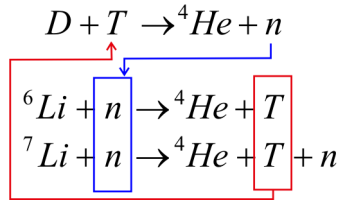


Figure 1.2: Schematic view of a fuel cycle in D-T fusion.

¹In most of the test breeding module designs lithium appears in a form of a lithium-based ceramic (Li_2O , Li_4SiO_4 , Li_2TiO_3 , Li_2ZrO_3) adjacent to a neutron multiplier (Be, Be-Ti, Pb-Li).

1.2 Fusion devices

Certain conditions must be achieved in order to ignite a D-T plasma and to keep it burning. A general way to describe these was introduced in 1955 and published two years later by John D. Lawson [8]. He defined the gain of a thermonuclear process as the *triple product* of the plasma density (n_e), the energy confinement time (τ_E) and ion temperature (T). To start a fusion process the so called Lawson criterion should be fulfilled, i.e. the triple product should exceed the minimal required value unique for each fusion reaction. In the case of deuterium-tritium fusion the Lawson criterion has the following form:

$$n_i T \tau_e \geq 3 \cdot 10^{21} \frac{\text{keV} \cdot \text{s}}{\text{m}^3} \quad (1.3)$$

The most common way to satisfy the Lawson criterion is presented by the *magnetic confinement fusion* (MCF) concept which is based on confining plasma by strong magnetic fields of the order of a few Tesla. The most popular type of MCF device - *tokamak* - received its name from the acronym of the Russian "Торондальная Камера с Магнитными Катушками" which is translated as "toroidal chamber with magnetic coils". An alternative approach is *inertial confinement fusion* (ICF) where plasma is formed by symmetrical irradiation of a fuel-containing target with multiple lasers or particle beams. A lot of details can be found in literature [9][10][11] and on the websites of the major ICF projects in the USA [12] and in France [13].

A schematic view of a tokamak is presented in Figure 1.3a. In the tokamak configuration poloidal and toroidal magnetic fields are designed in a way to maintain plasma inside a toroidal chamber. The toroidal field is generated by currents flowing through the external magnetic coils whereas the poloidal field is supported by plasma currents. Magnetic confinement allows relatively long pulses in the range of several seconds or even minutes in the case of superconducting coils. At present many tokamak facilities are contributing to the research on ITER related issues: JET [14], DIII-D [15], ASDEX-Upgrade [16], Tore-Supra [17], TEXTOR [18], JT-60U [19] followed by the upgrade to JT-60SA [20], NSTX [21] and many others. Table 1.1 contains basic information on the tokamaks where the studies presented in this thesis were carried out (TEXTOR, JET, Tore Supra) and two other machines for comparison. Figure 1.3b demonstrates the inner vessel of TEXTOR tokamak during a plasma discharge. Bright areas on the image correspond to *limiters*, which intersect the magnetic lines and thus protect other wall components. Advanced tokamak performance requires a *divertor* configuration, where the plasma edge is defined by a magnetic separatrix.

Significantly longer pulse length can be achieved in a *stellarator* where the complex magnetic field is created solely by external coils. The magnetic configuration in stellarators does not require the development of current drive techniques, which is essential for a steady-state tokamak type reactor. The largest superconducting stellarator in the world is the Large Helical Device (LHD) in Japan, where pulse

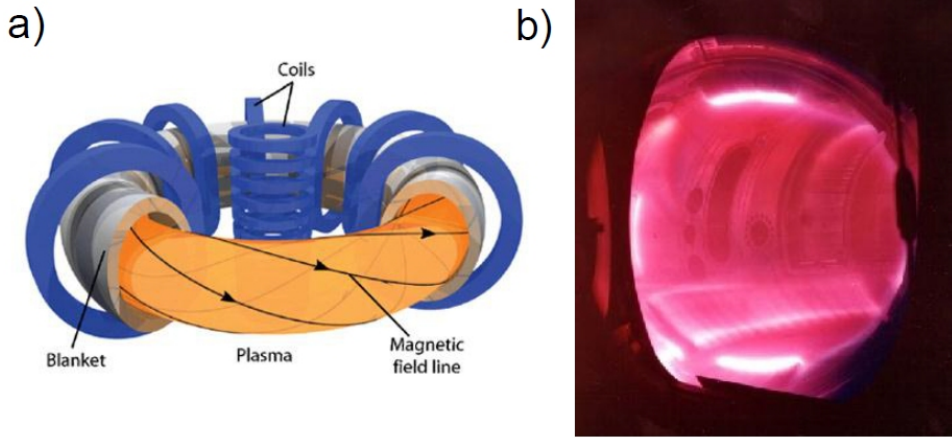


Figure 1.3: a) Basic principle of a tokamak; b) burning plasma in the TEXTOR tokamak.

lengths over 30 minutes have been achieved [22]. Another large stellarator Wendelstein 7-X is under construction in Greifswald, Germany [23].

As the most studied concept, the tokamak design was chosen for ITER. The configuration of the next step fusion device, DEMO, is still an open question. Many technological issues are the same for tokamaks and stellarators, e.g. plasma-facing components (PFCs), diagnostics, heating method, tritium breeding blanket, wall materials, superconducting coils, tritium cycle, control of steady-state operation. Thus many of the solutions found within the ITER operation limits could be later applied to a stellarator.

The work presented in this thesis deals with one of the most difficult technical issues, namely the selection of materials for PFCs. The work is primarily experimental and is based on the analysis and characterisation of test samples exposed in the TEXTOR, Tore Supra and JET tokamaks as well as samples treated in several laboratory setups.

Table 1.1: Comparison of various tokamaks.

Tokamak	Configuration	Major radius (m) / Minor radius (m)	Material of PFCs	Major scientific and technology mission
TEXTOR	limiter, dynamic ergodic divertor (DED)	1.75 / 0.47	Carbon / CFC	PMI and material testing
Tore Supra	limiter (water-cooled), superconducting magnets	2.25 / 0.7	CFC	Testing of actively cooled components; long pulse operation
JET	D-shape, divertor	2.96 / 0.96	Carbon / CFC, Be-evaporation	Fusion performance; divertor geometry
JET-ILW	D-shape, divertor	2.96 / 0.96	Be wall, W divertor	Operation with wall materials for ITER (activated phase)
DIID-D	D-shape, double-null divertor	1.66 / 0.67	CFC	Optimized fusion performance
ASDEX	D-shape, divertor	1.65 / 0.5-0.8	W-coated CFC	Fusion performance and high-Z wall

TEXTOR

TEXTOR is a medium size tokamak located at the Institute of Energy and Climate Research of Forschungszentrum Jülich, Germany [18]. The name of this tokamak stands for “Toroidal Experiment for Technology Oriented Research” and denotes the purpose of its construction in the early 1980’s. TEXTOR is a limiter machine with the toroidal belt limiter covering a total surface area of about 3.4 m². The dedicated design features (e.g. excellent access for diagnostics in the near-wall region and so-called *limiter locks* which allow for exposure of large-scale probes) make this machine well suited for studies of plasma-wall interactions (PWI) [24].

Figure 1.4 shows the inner view of the TEXTOR tokamak where the main locations of interest for this thesis are marked. The main plasma-facing components are: the Inconel *liner* (a bakeable vessel inside the vacuum chamber), RF antennas and an array of limiters made of graphite or carbon fibre composite (CFC). This implies that TEXTOR is a carbon wall machine. The toroidal belt limiter is composed of eight blades covered by 28 ALT-II (Advanced Limiter Test II) tiles each. The main poloidal limiter is represented by two groups of graphite blocks¹. The inner bumper limiter tiles protect the dynamic ergodic divertor (DED) installed in 2002 in order to improve the control over the plasma edge.

Tore Supra

Tore Supra is also a carbon wall limiter tokamak and is located at Cadarache, France - the Nuclear Research Centre of the French Atomic Energy Commission (CEA). The machine has superconducting magnetic coils that allow for steady-state plasma operation with plasma pulses several minutes long. Active cooling of wall components is implemented in order to protect against degradation of PFCs under high heat fluxes. Superconducting magnets and actively cooled components of the first wall make Tore Supra well suited for the study of physics and technology dedicated to long plasma discharges [27]. As can be seen in Figure 1.5, the main power handling component in Tore Supra is the Toroidal Pump Limiter (TPL). For this work samples of co-deposits were obtained from the deposition zone on the TPL removed from the tokamak within the DITS (Deuterium In Tore Supra) project [28].

¹During a couple of campaigns in the end of the 1990’s the poloidal limiter blocks on the top and bottom of the vessel were covered with a vacuum plasma sprayed (VPS) tungsten coating (about 0.5 mm) with a rhenium interlayer [25][26] on the top and bottom of the vessel. The limiters originating from that period were used as specimens in some studies presented in *Paper II*

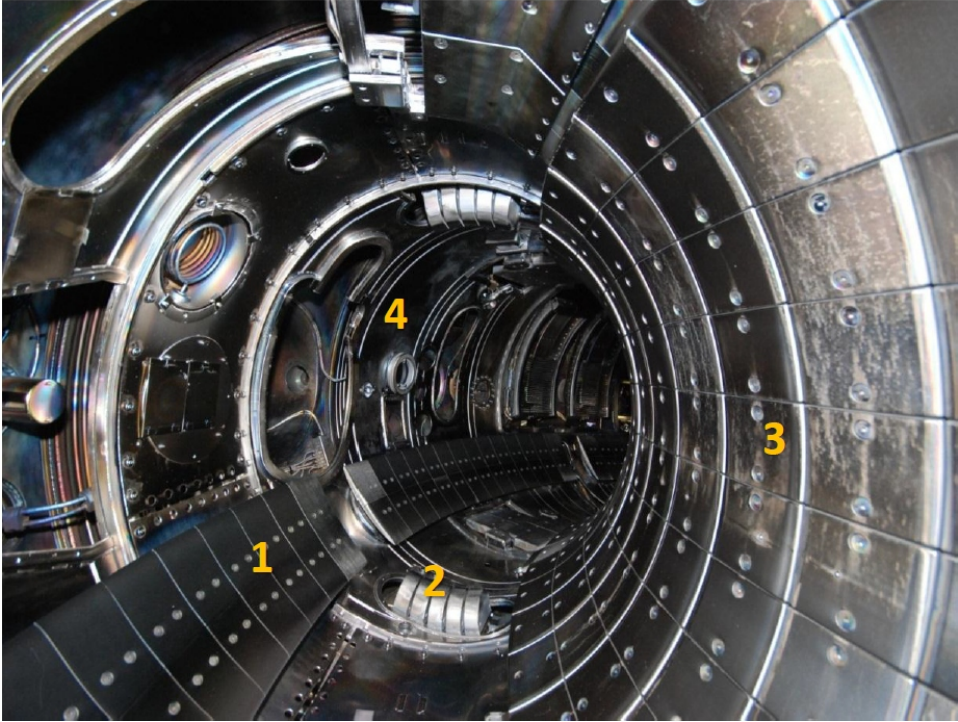


Figure 1.4: Toroidal view inside TEXTOR: 1) toroidal belt limiter covered by the ALT-II tiles, 2) main poloidal limiter, 3) inner bumper limiter, 4) Inconel liner.

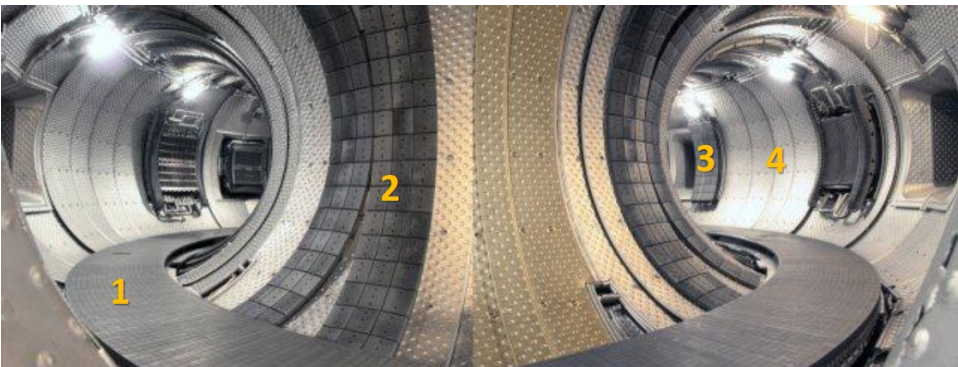


Figure 1.5: Toroidal view inside Tore Supra: 1) toroidal pump limiter (TPL), 2) inner bumper limiter, 3) outboard movable limiter, 4) vessel protection panels. ©Tore Supra

JET and JET-ILW

The Joint European Torus (JET) is the world's largest fusion experiment located at the Culham Centre for Fusion Energy, UK (see Figure 1.6). Unlike TEXTOR and Tore Supra, JET has a divertor configuration which allows testing operational scenarios for future ITER experiments. For this purpose the divertor has been changed several times during the last decade. Until 2009 JET was operated with a carbon wall (Figure 1.6 left). The next goal of the JET program was to study the combination of wall materials chosen for ITER operation in the activated phase, and the ITER-Like Wall project is aiming to answer most of the questions [29]. The refurbishment of the inner wall, which includes installation of beryllium and tungsten PFCs, was completed in May 2011 [30].

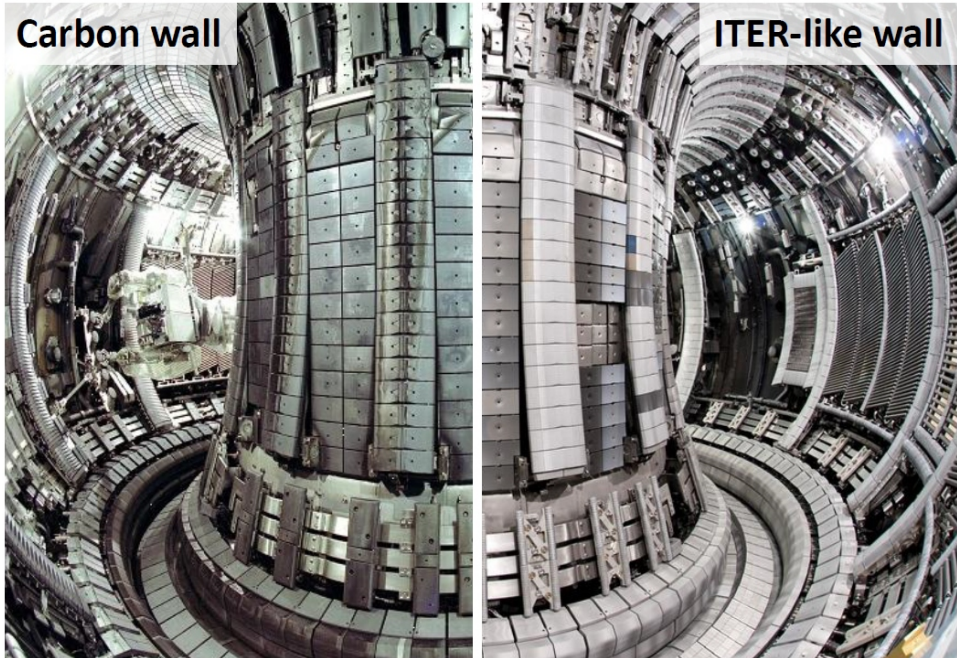


Figure 1.6: Toroidal view inside the JET vacuum vessel. To the left: the carbon-wall machine; to the right: after the ITER Like Wall installation. The image is composed of photographs protected by ©EFDA-JET

Chapter 2

Plasma-wall interactions

*We say that we will put the sun into a box.
The idea is pretty. The problem is,
we don't know how to make the box.*

Sebastien Balibar, Director of Research, CNRS

Despite all the work done on the improvement of plasma confinement, it will never be perfect. Plasma-facing components in every fusion device are exposed to high heat and particle fluxes from plasma. This makes the development of PFCs one of the key issues in fusion science and technology [31][32][33]. All components must withstand long-term operation and demonstrate a low level of dust production and fuel accumulation. A complete description of all processes in plasma edge is an extremely challenging task which requires both theoretical predictions, experimental observations and computational models. PWI processes are intensely studied in fusion devices, e.g. JET [34], TEXTOR [35][36], Tore-Supra [28], ASDEX [37], as well as in dedicated laboratory setups such as PISCES [38], JUDITH [39], Pilot-PSI [40] and the recently opened Magnum-PSI [41].

Understanding of the plasma-wall interactions provides the basis for developing new materials or choosing among existing ones. Compatibility between the fusion plasma and the surrounding materials is one of the main challenges for the construction of a fusion reactor. For the most exposed areas in a tokamak, the aim is to develop materials that are heat-resistant, thermally conductive, resistant to physical and chemical erosion and show low fuel retention [31]. The majority of the present-day machines operate with PFCs made of graphite or carbon fiber composites. However, the level of fuel retention and dust formation associated with the use of CFCs is not acceptable for reactor class devices, such as ITER. Many plasma-facing materials (PFMs) were tested throughout the previous decades and, as a result, the choice for the ITER wall consists of beryllium, carbon and tungsten for the initial hydrogen phase, while beryllium and tungsten are chosen for the activated phase of operation. The combination of these three elements should allow

for obtaining optimal parameters for the ITER operation, while materials for the next-step fusion devices are still under discussion.

2.1 Plasma-facing materials for ITER

ITER is designed to achieve a power gain of $Q = 10$ (here Q is the ratio of fusion energy released to the energy required to maintain the burning plasma), a fusion power of 500 MW and heat and neutron fluxes on the wall of above 1 MW/m^2 . An ideal material to deal with such loads would be:

- light enough to minimize pollution of the core plasma,
- non-reactive with plasma species to avoid generation of volatile products,
- an excellent thermal conductor (similar to CFC),
- resistant to thermal shocks,
- resistant to erosion processes,
- having a low activation and short-life products under neutron irradiation.

Such material does not exist. As a compromise, a combination of three materials was introduced in the ITER design [42][43][44]. The main chamber wall (700 m^2) will be covered with beryllium tiles, while tungsten (120 m^2) and carbon (35 m^2) will be used for the divertor (Figure 2.1). The most important thermo-physical properties of all three materials are summarized in Table 2.1. The divertor cassettes

Table 2.1: Properties of plasma-facing materials for ITER.

	Be	C (CFC)	W
Atomic mass [<i>amu</i>]	9.01	12.011	183.84
Thermal conductivity (λ) [$\frac{\text{W}}{\text{m}\cdot\text{K}}$]	190	200–500	140
Melting point [<i>K</i>]	1560	> 2500 (subl.)	3695
Thermal expansion [$10^{-6} \frac{1}{\text{K}}$]	11.5	0–4	4.5
Heat capacity [$\frac{\text{J}}{\text{kg}\cdot\text{K}}$]	1825	709	134
Behaviour under neutron irradiation	swelling	decrease of λ	activation
Major advantages	low <i>Z</i>	shock resistance	low erosion, low retention
Major disadvantages	melting	fuel retention, chemical erosion	activation, high <i>Z</i>

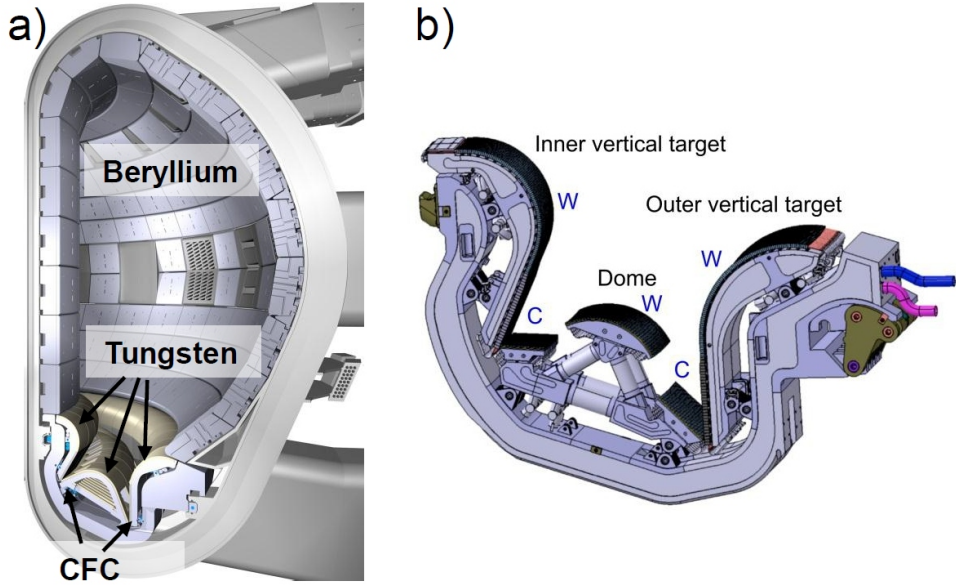


Figure 2.1: The present design of the ITER inner wall: a) poloidal cross-section of ITER vacuum vessel and plasma-facing materials, proposed for the initial phase of ITER operation; b) a divertor cassette for ITER.

(see Figure 2.1b) are planned to be replaced several times during the ITER life and CFC may be eliminated in future ITER divertor designs. It is worth mentioning that recently even the usage of carbon during the initial hydrogen phase of ITER operation has come under discussion and this material may be excluded completely from the ITER design [45][46].

Beryllium itself can withstand the designed power loads on the main wall of 1 MW/m^2 in normal operation [47]. The shaped Be tiles can be used even during the start-up and ramp down phases with power loads up to 7.5 MW/m^2 [48]. Thanks to its low atomic number (Z), beryllium ensures very low contamination of the plasma, and it also features lower fuel retention in comparison to carbon. The low melting point does not allow for using beryllium in the divertor, where power loads exceed 10 MW/m^2 and can go above 20 MW/m^2 during transient events and edge localised modes (ELMs) [33]. An additional advantage of beryllium is its oxygen gettering due to the formation of a stable oxide (BeO).

Tungsten has the highest melting point of all considered elements and has a high physical erosion threshold, which makes it a good choice for the divertor components, such as baffles, refractor plates etc. Unfortunately, tungsten loses ductility with temperature changes, and H and He bubble formation under neutron irradiation can cause material swelling [49].

Strike points of the divertor will be covered with CFC, chosen for its excellent heat conductivity and low Z . Carbon does not melt, has good power handling and thermal shock resistance, although its physical and mechanical properties degrade under neutron irradiation.

2.2 Material migration: erosion-deposition processes

When fluxes of charged and neutral particles from the plasma together with electromagnetic radiation meet any material, various processes occur on the surface and in the bulk. Some incident particles are reflected and return to the plasma with a minor loss of kinetic energy. In most cases more advanced PWI processes take place, such as physical sputtering, chemical erosion and sputtering, melting, sublimation and brittle destruction [50][51][52]. A schematic view of the basic processes which take place at the plasma-wall interface is shown in Figure 2.2.

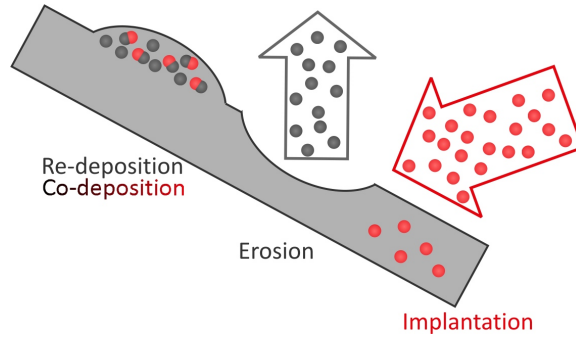


Figure 2.2: Scheme of plasma-surface interactions

The removal of wall material under impact of plasma fluxes, erosion of materials, results both in the reduction of the material lifetime and plasma contamination. Erosion of PFCs includes a number of processes, of which the following ones are the most important:

Physical sputtering. This mechanism denotes the removal of atoms from the surface as a result of energy transfer between the incident energetic particles and surface atoms. Physical sputtering occurs for any material and its efficiency (*sputtering yield*, i.e. number of ejected particles per projectile) depends on the incident angle and energy of projectiles, the masses of the ion and target atoms and the surface binding energy [53][54]. A common approximation for physical sputtering is given by the binary collision model where the masses of the interacting atoms play the dominant role. The energy transfer E between the incident atom and the surface material is then defined by:

$$E = \gamma E_0 (\cos\theta)^2 = \frac{4M_1 M_2}{(M_1 + M_2)^2} E_0 (\cos\theta)^2 \quad (2.1)$$

where E_0 denotes the initial energy of the projectile, M_1 and M_2 are the masses of the particles, θ is the scattering angle. Physical sputtering will occur only if E_0 exceeds a threshold value, which depends on the surface binding energy U_s :

$$E_{th} = \frac{1}{(1-\gamma)\gamma} U_s = \frac{(M_1 + M_2)^4}{4M_1 M_2 (M_1 - M_2)^2} U_s \quad (2.2)$$

Examples of the erosion yields for fusion PFMs under the impact of D^+ ions are shown in Figure 2.3. It can be seen that for metals (beryllium and tungsten) the experimentally found values for the sputtering yield are in a good agreement with the modelled data, whereas the behaviour of carbon for incident ions with low energies does not follow the predictions. This deviation from the physical sputtering model is attributed to chemical erosion of carbon.

Chemical sputtering and erosion. Chemical erosion refers to the reaction of the target and plasma species towards the formation of volatile products.

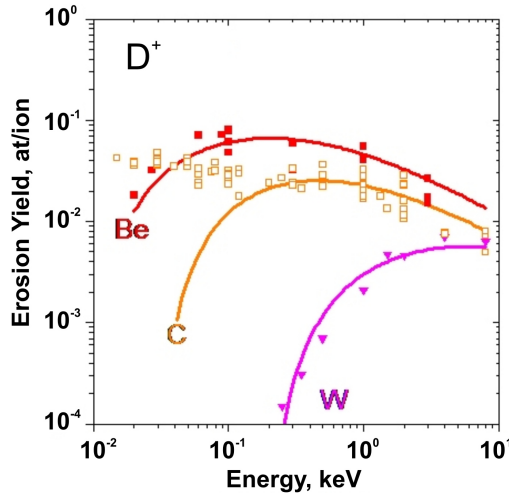


Figure 2.3: Erosion yields of beryllium, carbon and tungsten under the impact of D^+ ions. Solid lines show theoretical predictions for physical sputtering. Dots correspond to experimental results [31].

Unlike physical sputtering, chemical processes strongly depend on the type of material and on the surface temperature. From all considered wall materials carbon is the most vulnerable to chemical erosion. When hydrogen isotopes bombard the carbon wall, various hydrocarbons may be formed and then thermally released to the plasma. Similar processes occur under the impact of oxygen towards the formation of CO and CO₂. Tungsten can also be chemically eroded at high temperatures and in the presence of oxygen impurities, leading to the formation of volatile oxides WO₂, WO₃ [55][56].

Melting and sublimation. Under high heat fluxes the surface temperature may exceed the melting point of the material. The molten metal can either be ejected into the plasma in the form of small droplets or recrystallise, producing an area with new physical properties. Carbon does not melt but goes directly from the solid to the gaseous state (*sublimation*). However, under high power loads brittle destruction may take place [57].

After entering the plasma, the eroded particles are eventually re-deposited on the vessel wall, unless they are pumped out. Re-deposition may occur promptly on surfaces close to the origin of erosion, but in most cases eroded particles are transported along the field lines over long distances. Deposited layers undergo the same plasma-wall interaction processes as a virgin surface and can be eroded again. Finally the balance between incoming and outgoing particle fluxes defines the net erosion or deposition for this area. Net erosion is typically observed at the strike points in the divertor. Areas with a net deposition can be seen in low-flux zones on the divertor and limiter plates, but the thickest deposits are usually found in areas without direct plasma contact, i.e. gaps in castellated structures or in pumping ducts [34][58].

The formation of deposits changes the chemical and physical properties of the surface. Fuel atoms and plasma impurities are co-deposited together with the eroded wall species forming new mixed materials, as well as chemical compounds [59][60]. The influence of co-deposition is enhanced if several different plasma-facing materials are used. This may be decisive for fuel retention, especially in the presence of carbon.

Deposited layers even in machines with only carbon PFCs have a complicated structure and a mixed chemical composition. Such layers were named “tokamakium” in the 1980’s [61]. The combination of materials chosen for ITER (Be-W-C and Be-W) had never been tested in tokamaks and may lead to the formation of mixed alloys with not well-defined properties [62]. The first large-scale test is ongoing in the frame of the ITER-Like Wall project at JET [29][63]. JET-ILW, with beryllium wall components in the main chamber and a full tungsten divertor, started operation in August 2011 and the first results have already been reported [63]. For example, plots in Figure 2.4 show the evolution of carbon and beryllium fluxes in the divertor during JET operation with the ILW. The author of this thesis was responsible for processing these data. The results are included in [64][65].

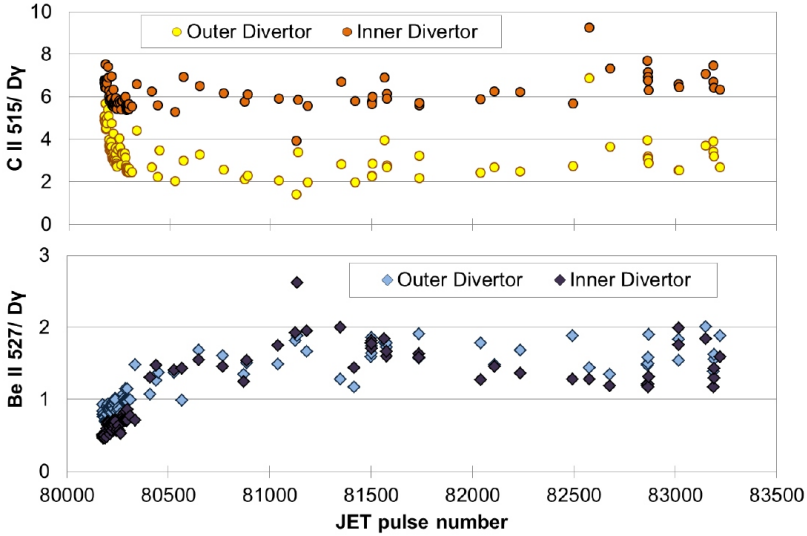


Figure 2.4: Evolution of the flux ratios C II / D_γ (upper plot) and Be II / D_γ (lower plot) fluxes in the divertor during the JET operation with ILW.

2.3 Dust in fusion devices

In fusion science and technology “*dust*” denotes all erosion products resulting from PWI processes and covers a range of particle dimensions from a few nanometres to millimetres [66]. During the operation of a tokamak, small-size particulates are produced and accumulated inside the vacuum vessel. In present-day machines the release of dust into plasma plays a relatively minor role and it is not an operation hazard. However in a reactor-class device, i.e. ITER, the formation and accumulation of dust may become a serious economy and safety issue. The main concern is related to a possibility of explosion in the case of oxygen or water contact with hot dust in the event of an air or water leak. A risk of mobilization and release of radioactively contaminated products by an explosion must also be taken into account. Finally, degradation of diagnostic or pumping components may cause operational problems even before any safety limit of dust and tritium accumulation has been reached. Several mechanisms of dust production have been identified:

Flaking. Most of the eroded material in tokamaks is typically found in the form of re-deposited layers on PFCs, especially in carbon wall machines. Under thermo-mechanical stresses these deposits may flake, peel-off and form dust agglomerates. Exposure of deposits to air or water vapour (i.e. during tokamak venting or air leaks) may lead to additional stratification of layers and enhanced liberation of flakes [67][68][58].

Arcing. Electrical arcs of short duration (millisecond range) can occur in a fusion device during the start-up phase between the plasma and the wall, leading to erosion of wall material. The material release by arcs depends on the thermal conductivity and the melting point [69]. For a carbon wall, the impact of arcing on the total erosion rate is much smaller than that of physical and chemical erosion, but in the presence of a metal wall or metal-containing components, arcing becomes an important source of dust particles [70][71].

Melting. Another source of dust relevant for metal PFCs is melting under extreme power loads (i.e. ELMs), melt layer motion and eventually splashing of droplets. Examples of metal droplets found in the TEXTOR tokamak are shown in Figure 2.5a,b. The issue of metal dust (beryllium and tungsten) formation is still to be properly addressed and a major study will be carried out in connection with ex-situ examination of components from the ITER-Like Wall operation of JET [63].

Brittle destruction. Brittle destruction of carbon may occur under localized high power loads and can lead to dust production. The relevance of this mechanism in fusion devices is still to be proven [68][72][57]. There is evidence of brittle destruction under off-normal events in fusion devices (*Paper I*) but the extent of the phenomenon is still to be determined.

Mechanical source of dust. Some larger debris can and will be produced during in-vessel installation works in shutdown periods (Figure 2.5c).

Dust generation mechanisms, conversion of deposited layers to dust, dust transport and mobilisation still need to be studied in greater detail. Now dust surveys are regularly performed on most of the larger fusion experiments, i.e. TEXTOR [67] [68] [*Paper I*], ASDEX-Upgrade [71], Tore Supra [74], JT-60 [75], JET [34]. The work presented in this thesis includes studies of dust in carbon-wall machines: TEXTOR and Tore Supra (*Papers I-IV*).

The size distribution of dust particles also plays an important role. Large debris, as shown in Figure 2.5b, are usually too heavy to be mobilized by plasma. Dust pieces of such scale ($> 100 \mu\text{m}$) tend to remain on the bottom of the vacuum vessel and can be removed by vacuum cleaning during the shutdown period. Small-size dust ($< 1 \mu\text{m}$) typically has a high sticking coefficient and may present more difficulties for the cleaning procedure.

As can be seen from the list of mechanisms of dust production, dust particles result from various erosion processes. The present administrative limits for in-vessel dust accumulation in ITER are based on a safety analysis. Two dust limits are set: the cold dust limit (1 ton) refers to the total amount of mobilized dust and can hardly be of any concern; the hot dust limit (6 kg of C, 6 kg of Be, 6 kg of W) takes only into account dust residing on hot surfaces. In the most restrictive estimations it can be reached in less than 100 ITER discharges [76].

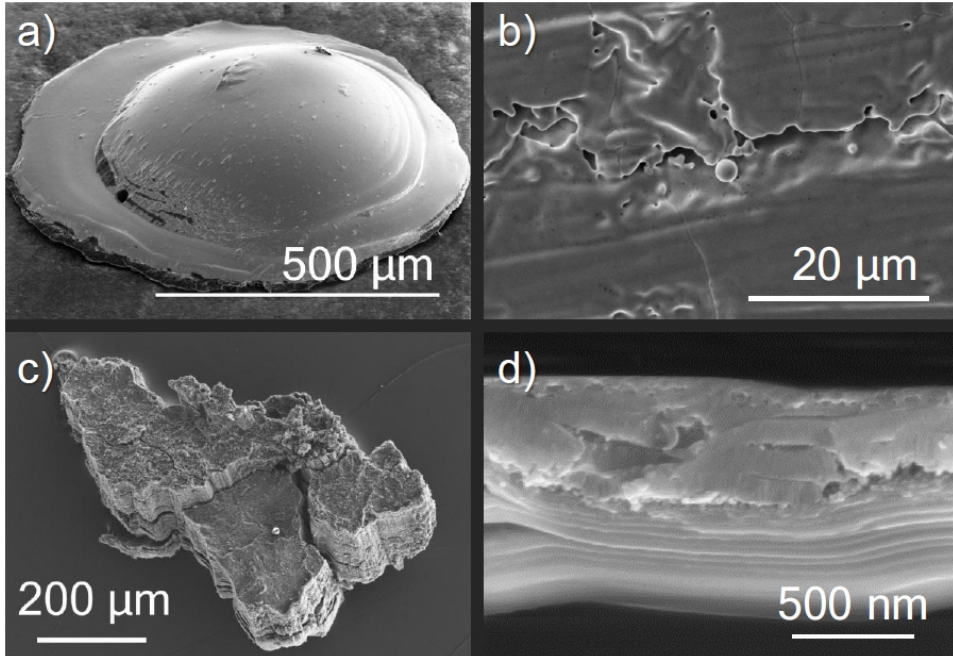


Figure 2.5: Examples of large-scale debris and fine dust observed in the TEXTOR tokamak: a) a droplet of molten metal (Ni-Cr-Fe) [73]; b) a tungsten droplet; c) carbon dust, possibly resulting from brittle destruction; d) splitting of carbon deposits into nano-scale dust-forming strata. Photos a), c) and d) were presented in *Paper I*

The ratio between the dust production and the gross erosion is often called the *conversion factor*. Its assessment is important for the best possible predictions for ITER. However, the determination of this parameter is associated with several uncertainties:

- Some of dust species are originating from the mechanical damage to the in-vessel components and should not be included in the conversion factor;
- Ultra-fine dust sticks to PFCs and tools, used for dust collection, making it impossible to determine the total amount of dust particles;
- A part of the eroded material, especially in the case of carbon, is pumped out, which causes difficulties in the estimation of the total erosion yield.

In *Paper I* the conversion factor was assessed for TEXTOR. It is about 0.5% which is lower than the previously reported values for Tore Supra: 7%-8% [77]. This is probably attributed to the difference in the operation of the two machines,

e.g. plasma heating. High edge temperature in Tore Supra strongly increases the erosion yield. (*Note:* In *Paper I* an alternative definition of the conversion factor is used. It denotes the ratio of the total eroded material to the amount of loose dust and in case of TEXTOR is 200-400)

2.4 Fuel inventory

In-vessel retention of fuel refers to all hydrogen isotopes remaining in PFCs. It becomes extremely important when tritium is considered as a fuel [78][79]. In-vessel retention of tritium must be monitored and minimised both due to economical and safety reasons. Only about 1-2% of the injected tritium will be burnt in the fusion reaction while most of it will be recycled by the fuel plant. ITER, as a machine designed for D-T fusion, has an administrative in-vessel limit for tritium retention of 700 grams [76]. Figure 2.6 shows the estimation of in-vessel tritium retention in ITER for different combinations of PFMs. From the extrapolation of present experimental data from TFTR and JET [80][81] it follows that for a full carbon wall the limit of 700 grams would be reached already in 20–50 full power discharges. Predictions for a mixed and all metal wall show that a few hundred full-performance discharges (pulse duration 400 s, 50%-50% D-T, $Q = 10$) will be enough to reach the tritium retention limit [82]. The safety limit for in-vessel tritium inventory is marked (700 g). The double-sided arrow indicates a reduction in fuel inventory by one order of magnitude, which was also observed in operation of JET-ILW [63]

Under normal vacuum conditions, remaining gas in the vessel can be adsorbed by wall materials. The weakly bound volatile species can be removed thermally and at any given surface temperature there will be an equilibrium between the adsorption and desorption of particles. In the case of plasma devices, where plasma-wall interaction and material migration are decisive, the fuel retention during a single plasma discharge can be estimated through the global particle balance [83]. These calculations cannot be used for the prediction of the long-term fuel retention where disruptions and wall-conditioning between discharges play their role. Post-mortem analysis of the wall components, and especially in the areas with net deposition, is another approach for the long-term retention studies. Now a big selection of fusion experiments with a carbon wall provides a broad database for these types of PFMs. There are several pathways leading to the in-vessel accumulation of fuel [84]:

Co-deposition. The chemical sputtering and erosion of carbon leads to the production of hydrocarbons and eventually their re-deposition on the wall and in remote areas, i.e. pumping ducts in divertor machines. As a result, fuel-rich inhomogeneous layers are formed. Co-deposition was recognised as a dominant mechanism of fuel retention in carbon-wall machines. Experiments in metal surroundings (ASDEX-U, JET-ILW) should further clarify the role of carbon in the total fuel retention and recent reports from ASDEX show a significant reduction of the total dust and the retained fuel in the machine [85].

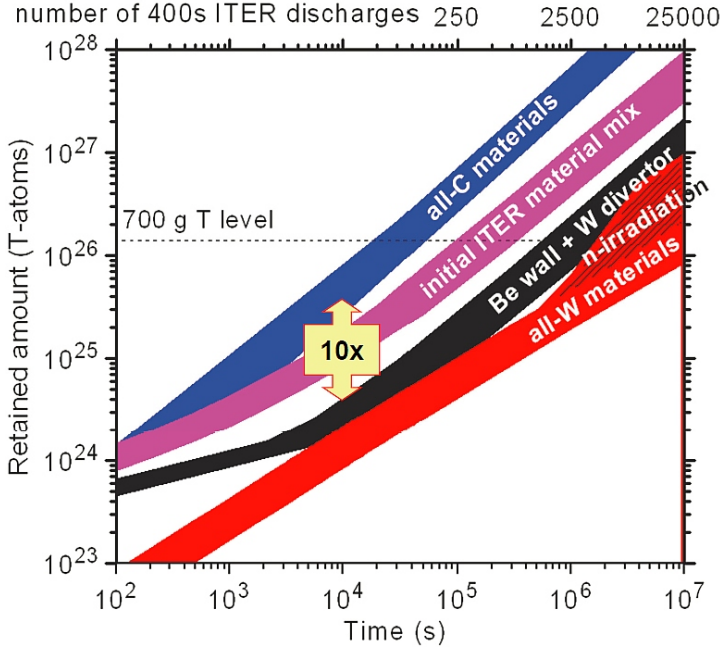


Figure 2.6: Estimation of in-vessel tritium retention in ITER for different combinations of PFMs: all-C (blue line), all-W (red line), initial material choice CFC/W/Be (magenta line) and W/Be option (black line) [76].

Implantation, followed by diffusion and trapping. Energetic particles can be implanted into solids and after a series of scattering events they can remain in the material [86]. For the typical range of hydrogen energy in a tokamak boundary plasma (0.1 – 1 keV) the implantation depth in carbon and beryllium is 3 to 30 nm, and it is even smaller for higher Z materials [87]. Further diffusion of implanted ions deep under the surface (several μm) and possible trapping strongly depend on the material properties [88].

Neutron-induced effects. Fuel retention can also be enhanced due to neutron irradiation which is unavoidable in D-T fusion. An example of such retention would be tritium retention in helium bubbles, which are formed in beryllium under the impact of neutrons.

The problem of the fuel inventory is related mainly to tritium retention, but the experimental domain is usually limited to working with a more common isotope of hydrogen, e.g. deuterium which is used in present-day tokamaks.

Chapter 3

Removal of fuel and co-deposits

As described in the previous chapters, material migration, especially in the presence of carbon, leads to dust formation and fuel retention, which eventually may hinder the fusion reactor operation. The necessity of in-situ detection and cleaning of deposits was recognised decades ago [89] and as long as carbon fibre composites remain the material of choice for high heat flux regions in the ITER diverter this topic will be of significant importance. The frequency of fuel removal will depend on the rate at which codeposits are built up and on the concentration of fuel in the layers [90]. The proposed methods for in-situ fuel removal are:

- thermal removal of fuel and co-deposit,
- photonic cleaning using lasers and flash-lamps,
- oxidative, chemical and gas-assisted methods,
- ion cyclotron wall conditioning.

Table 3.1 at the end of this chapter summarises the studied materials and experimental conditions for fuel release studies at TEXTOR.

3.1 Thermal methods

When a solid material is heated, volatile species leave the surface. These are adsorbates or products originating from the decomposition of larger molecules. This basic method can be used to release hydrocarbons and trapped hydrogen isotopes from the PFCs, so-called *baking*. However, thermal desorption of hydrogen isotopes requires heating up to high temperatures (above 1000 K) [91] which is not feasible in ITER. Thermal expansion of PFMs and joining materials limits the maximum allowed baking temperature of the main wall to 513 K, and to 623 K for the divertor [92][93]. Also, the chemical and physical properties of the mixed layers will lead to changes in the efficiency of baking [94]. The question whether a long-term annealing of deposits at this rather moderate temperature gives an efficient release of

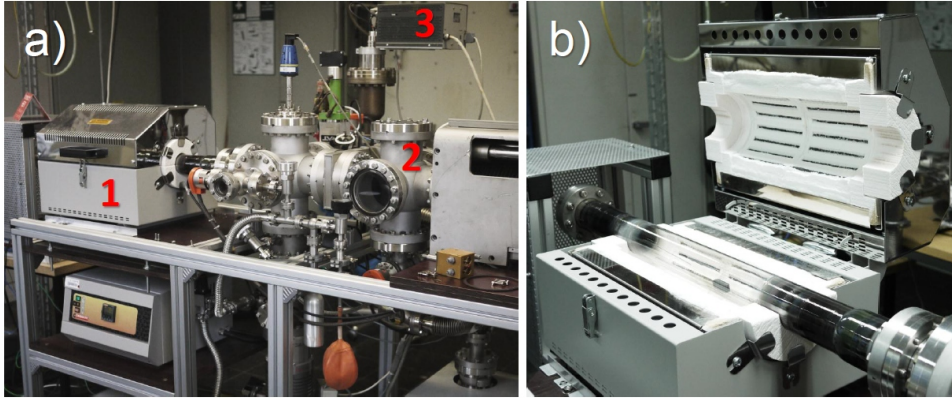


Figure 3.1: TDS facility at FZ Jülich: a) the TDS setup consisting of an oven (1), a chamber for a sample exchange (2) and a mass analyser (3); b) an open oven with a graphite sample placed inside the quartz tube.

hydrogen isotopes is addressed in *Papers I, II* and *IV*. The samples were outgassed in a temperature-programmed oven which is shown in Figure 3.1.

3.2 Photonic methods

Laser technology is employed in many industrial applications [95], medicine [96][97], food processing and even for cleaning delicate surfaces of archaeological objects and pieces of art [98]. Lasers are selected for surface cleaning purpose due to a high level of controllability and selectivity with a high removal rate sufficient in most applications. In relation to PFCs in fusion devices, lasers were initially proposed for desorption of hydrogen isotopes from the PFCs as an in-situ diagnostic tool [99]. Now laser-induced desorption of fuel species from the deposits [100] and removal of the whole co-deposited layer by exposing it to an intense laser light [101] are discussed. Laser techniques have several strong advantages over other methods. Light from a laser can be transported by optical fibres, making it possible to control the process via remote handling [102]. Since co-deposits on PFCs have different physical properties from those of the substrate, it is possible to define threshold values for laser parameters and thus avoid damage to the bulk material. Due to the small size of a laser spot the light could access challenging areas such as gaps in castellated structures [103].

Drawbacks of photonic methods are strongly related to the most appealing features of lasers. Due to the small area of laser-surface interaction treatment of the whole reactor vessel would take a long time, especially in complex areas such as louvers, curved surfaces and zones shadowed from the direct plasma line-of-sight. Deposited layers are not uniform and their chemical composition may vary, hence

laser parameters must be mild enough to allow for removal of thin deposits. A repetitive treatment of areas with thicker deposits will be required, making this method even more time consuming. Alternatively a feedback control method, i.e. spectroscopic monitoring of the desorbed and ablated species, should be implemented. Additionally the generation and composition of ablated products have been very rarely addressed in the past. Laser-assisted cleaning was also applied for the regeneration of mirrors exposed in JET within the First Mirror Test (*Paper VI*).

Issues related to the impact of the laser beam on the modification of cleaned surfaces are treated in the thesis in *Papers II, IV and VI*. The use of a laser under ablation conditions results in fuel and co-deposit removal. Preliminary studies have shown that this process is associated with the generation of ablation products: solid debris and gaseous species [101]. Systematic studies have been undertaken in order to address these issues (*Paper II*).

3.3 Plasma-assisted methods

A glow discharge in various gases (e.g. H_2 , D_2 , He, O_2 , N_2) can be used for removal of fuel and co-deposits from PFCs. Thermal oxidation of deposited carbon films results in the production of volatile oxides leading to an effective removal of fuel and carbon [104]. However, the removal rate is reduced significantly when the treated layer contains impurity atoms (e.g. Be [105][106], B [107][108], W [109]). Oxidation experiments at TEXTOR have shown that this method is effective only at a surface temperature exceeding 570 K, which is approaching the ITER operating temperature [108][110].

There is uncertainty about the applicability of oxidative techniques in the ITER environment [93]. Already during the non-activated phase of ITER operation there is a risk of oxygen-related damage to the wall (i.e. formation of BeO layer and/or impact on volatile tungsten oxides) and embedded diagnostics, while the use of oxidative techniques is restricted during the D-T phase of ITER operation due to production of tritiated water (DTO).

Nitrogen-assisted methods are studied as an alternative to the oxidative techniques. Studies in with N_2 injection indicated a very low fuel removal rate [111][112], while more optimistic results were obtained with NH_3 but only under laboratory conditions [113].

3.4 Ion cyclotron wall conditioning

Ion cyclotron wall conditioning (ICWC) is one of the proposed fuel removal techniques which is fully compatible with the presence of the magnetic field and is considered for the use at ITER [93][114]. Nevertheless, no detailed surface analysis of wall components after high power radio-frequency (RF) pulses has been carried out so far.

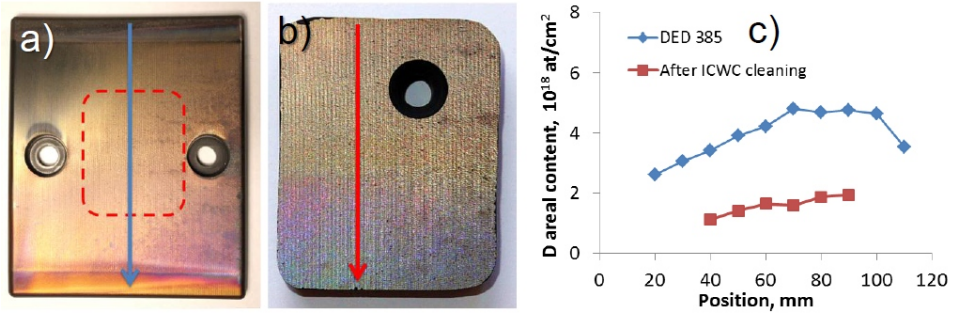


Figure 3.2: a) DED tile as retrieved from TEXTOR. The contour line corresponds to the area chosen for ICWC cleaning; (b) specimen sectioned from the tile and exposed to ICWC pulses; (c) deuterium content on the DED tile before after ICWC pulses. The direction of scan is marked in (a) and (b) [116].

A series of experiments has been started at TEXTOR in order to provide some information on the response of the fuel-rich deposits to ICWC cleaning. Several DED tiles (see Figure 1.4) were retrieved from TEXTOR after several years of operation and studied in detail with ion beam analysis for deuterium content. One such pre-characterised tile (Figure 3.2a) was exposed in TEXTOR during the multi-pulse operation in hydrogen (H_2 -ICWC) experiment [115]. Figure 3.2b shows a piece of that tile after exposure to ICWC pulses (the hole was drilled for sample attachment) and plots in Figure 3.2c show the deuterium content measured before and after the experiment [116]. One perceives the decrease in fuel content following the ICWC in hydrogen. The drop is by a factor of more than two. These are the first data of that kind obtained after cleaning a long-term wall component from a tokamak. The results are encouraging but still more detailed research is needed especially when it comes to the release of fuel from remote areas where the greatest deposition and fuel inventory has been observed. They are not accessible by ICWC.

3.5 Mechanical cleaning

All cleaning methods briefly described above have serious limitations even when used ex-situ. This is related to the complex nature of the deposits. Therefore, it was decided to check systematically the efficiency of a mechanical approach. Two very simple techniques were employed for the cleaning of mirrors: an ultrasonic (US) bath and polishing (*Paper VIII*).

For the US cleaning the mirrors were placed in an ultrasonic bath which is routinely used for cleaning various components for JET. A set of mirrors was placed in isopropanol and treated by ultrasound for almost one hour. For most samples US cleaning did not lead to a significant recovery in reflectivity.

Polishing was used as the next step in the cleaning procedure. For the most flaky and poorly attached deposits manual buffing was used. After that the cleaning was continued on the standard automatic polishing system, which allowed for simultaneous treatment of up to 3 mirrors with a force applied individually to each mirror. Polishing was done in steps lasting two minutes each until the initial (pre-exposure) reflectivity was reached. A measure of cleaning efficiency in this case is the time required to reach the pre-exposure state. An important factor affecting the efficiency of cleaning was the type of a diamond paste grain size ($1\mu\text{m}$, $3\mu\text{m}$).

Table 3.1: Fuel removal methods: summary of experimental conditions. (Adapted from *Paper IV*)

Technique	Experimental conditions	Treated materials
Thermal	Baking in vacuum: – 623 K, 2 h or 72 h – 573 K, 1 h	– ALT-II (D/C \sim 0.09–0.12) – main poloidal limiter (D/C \sim 0.03) – RF-antenna protection (D/C \sim 0.033–0.05)
Oxidation in air (laboratory)	– 573 K, 2 h – 573 K, 10 h – 823 K, 1 h	– deposits on the collector probe (D/C \sim 0.1–0.12)
Plasma in TEXTOR	– He - O ₂ RF glow – H ₂ - N ₂ discharge by ICRF: 25 shots, 40s total	– a-C:D laboratory films (D/C \sim 0.6) – B/C-D layers after boronisation in TEXTOR
Plasma in TOMAS (laboratory)	H ₂ - N ₂ glow, RF-assisted, 1h and 2h, T_{target} 313-563 K	– a-C:D laboratory films (D/C \sim 0.5–0.6)
Photonic (ablation)	ruby laser (694.3 nm) pulse duration 20 ns energy density \leq 14 J/cm ²	– deposits on ALT-II (D/C \sim 0.09–0.12) – deposits on VPS-W coated poloidal limiter (D/C \sim 0.12)
Photonic (desorption)	Nd:YAG laser (1064 nm) pulse duration 3 ns power density \leq 100 kW/cm ²	– a-C:D laboratory films (D/C \sim 0.55) – Carbon deposits on a tungsten plate after exposure in TEXTOR (D/C \sim 0.1) – ALT-II (D/C \sim 0.1–0.12)
ICWC	– H ₂ - ICWC discharges: 490 pulses pulse duration 0.5 s	– deposits on DED limiter tiles (D/C \sim 0.1)

Chapter 4

Surface morphology studies

There are three important issues which are common for all PFC cleaning and fuel removal techniques:

- the efficiency of the selected method,
- the impact on surface modification,
- the impact on dust generation.

In order to monitor the gas phase and surface properties and to improve the understanding of the impact of cleaning methods on the PFCs, a spectrum of analysis methods is employed. All methods listed below were used during the work on the thesis.

4.1 Electron microscopy

Material modification occurs on different scales. In the case of the macroscopic effects, damaged components can be assessed by visual inspection, but more commonly magnifying tools are required. Objects in the millimetre range can be successfully studied with the help of a conventional optical microscope. Due to diffraction effects the best achievable resolution with an optical microscope is $0.2\ \mu\text{m}$, which is obviously not enough in studies of nanometre scale structures. Electron microscopy helps here, providing not only a magnified image of the studied sample but also additional information on the chemical composition and physical structure.

Two types of electron microscopes were used during the work on this thesis: transmission and scanning electron microscopes.

Transmission electron microscopy

A typical Transmission Electron Microscope (TEM) uses a high voltage (100 – 1000 keV) electron beam to produce images of crystals and metals at the molecular level. Electrons have a much lower wavelength than visible light and this makes it possible

to achieve magnifications of up to two million times, i.e. three orders of magnitude higher than with a light microscope. In a typical TEM, an electron beam is focused by electromagnetic lenses on the studied material and the transmitted electrons hit a fluorescent screen below the sample. At this point, the electrons are converted to light and an image is formed.

Dark areas in the image correspond to regions on the sample where fewer electrons were able to pass through (either absorbed or scattered upon impact); the brighter areas are where more electrons were transmitted. Moving the sample and varying the amount of transmitted and scattered electrons in these areas allows the study of the material structure.

A sample for TEM studies must be thin enough to allow penetration by the electron beam. The preparation of samples for TEM studies often includes slicing of material into very thin films. In *Papers I* and *II* some samples of ultra-fine dust were studied after collection on the dedicated TEM holders, so called TEM nets, made of fine copper wires and a carbon ultra-thin film as a support for the studied specimen.

Scanning electron microscopy

A Scanning Electron Microscope (SEM) produces a magnified image by using electrons. The electrons in the beam originate from an electron gun at the top of the microscope, accelerated to about 5 – 20 keV and focused on the sample. Once the beam hits the sample, high-energy electrons will be either elastically scattered from the surface or interact with the atoms causing emission of electromagnetic radiation and secondary electrons. All three signals – secondary electrons, backscattered electrons and X-rays – are commonly evaluated in SEM. Secondary electrons have a relatively low energy and, when produced deeper in the sample, can be absorbed by the material atoms. Only the secondary electrons which were generated in the first few nanometres of the surface can reach the detector and contribute to the secondary electron image (SEI). Brighter areas on SEI correspond to parts of the sample ‘lifted’ towards the detector. Backscattered electrons have much higher energies and give information on the atomic number contrast of the surface elements. Heavy elements backscatter electrons more strongly and correspond to brighter areas on the backscattering electron image (BEI). Thus SEI (Figure 4.1a) shows the morphology and topography of the sample, while BEI (Figure 4.1b) indicates the composition of the surface. Characteristic X-rays give further information on the elemental composition of a specimen. Detection of X-rays is a base for techniques called energy-dispersive X-ray spectroscopy (EDX or EDS), wavelength dispersive X-ray spectroscopy (WDS) or electron microprobe.

In this thesis SEM was used in every step of the study to monitor the surface modification of PFCs due to exposure to plasma or implementation of cleaning techniques.

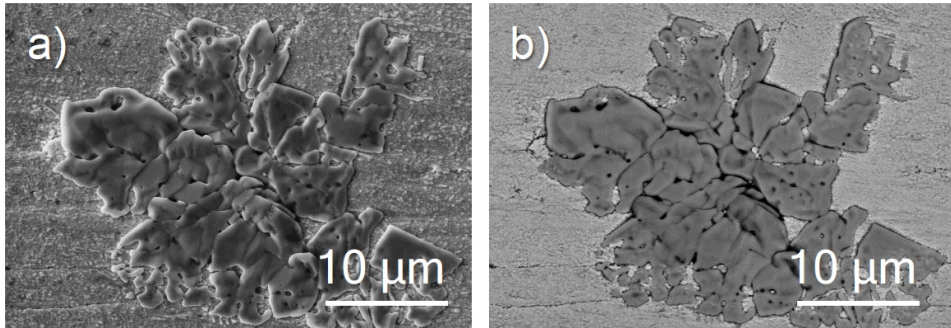


Figure 4.1: Examples of SEM images of tungsten oxide (WO_2) on the castellated W limiter from TEXTOR: a) Secondary electron image (SEI); b) Backscattered electron image (BEI).

4.2 Surface profilometry

A profilometer is an instrument which is used to determine topological features, i.e. the roughness of various surfaces. In a traditional contact profilometer a diamond stylus is used to achieve a vertical resolution in the nanometre range. An optical profilometer is a non-contact method where the stylus is replaced with a laser beam or a light beam, employed in confocal microscopy. A stylus profilometer and a confocal microscope were used in this work for studies of the craters resulting from laser irradiation (*Paper II*). Typical profiles of the laser-produced craters in the graphite surface are shown in Figure 4.2.

The profilometer Dektak 6M is capable of vertical scans in the range from 5 nm to 500 μm with a resolution of 0.1 – 4 nm. The horizontal resolution directly relates to the scan length (limited between 50 μm to 30 mm) and number of data points per scan (300 data points per second). The working principle is the following: a sample holder is mechanically moved in the horizontal plane beneath a diamond-tipped stylus and the surface variation causes the vertical translation of the stylus. This vertical movement is converted into a digital format through a high precision analog-to-digital converter.

A confocal microscope enables reconstruction of 3D structures. Unlike the conventional microscope, where the uniform light on the sample provides a high level of noise, a confocal microscope eliminates the out-of-focus signal by using a scanning point of light instead of full sample illumination. The light reflected from the surface is filtered by blocking the out-of-focus light. The increase in resolution comes at the expense of a decreased signal intensity, thus longer exposures at each point are needed.

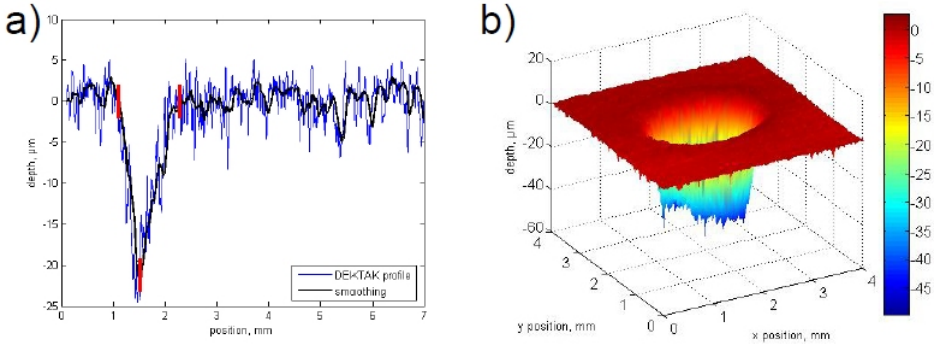


Figure 4.2: Profilometry of laser-produced craters in graphite: a) 2D image, stilos profilometer Dektak 6M; b) 3D image, confocal microscope STIL MicroMeasure.

4.3 Ion beam analysis

Ion Beam Analysis (IBA) - this general term denotes a large number of analytical techniques which are based on the interaction between a high-energy ion beam and the target material [117] [118]. When a charged projectile strikes the sample it interacts at either the atomic or the nuclear level with the material atoms. This collision can lead to changes in the kinematic parameters of the projectile and to the emission of particles or radiation, the energy of which characterises the elements of the sample material. Depending on the chosen method, IBA can provide information on the elemental composition, absolute atomic ratios in compounds, areal density and thickness of films, depth profiles up to several microns for a given element which makes it a very powerful tool for fusion material studies [119][120][121][122].

In this thesis most IBA studies were carried out at the Tandem Laboratory at Uppsala University [123]. Some specific studies were performed in the laboratories at FZ Jülich (Germany), University of Sussex (UK), VTT (Finland). The various ion beam analysis methods relevant to the thesis are listed further in this section and are summarized in Table 4.1.

Rutherford backscattering spectroscopy

Rutherford Backscattering Spectroscopy (RBS) is based on the detection of the charged particles elastically scattered by the nuclei of the analysed sample. It allows to distinguish atomic masses of elements and to determine the depth profile distribution as a function of the detected energy. RBS with light projectiles (typically $^4\text{He}^+$ or $^3\text{He}^+$ ions) became one of the most common IBA techniques in application to fusion materials. Backscattering only occurs when the mass of the incoming ion is smaller than the target atom. This makes hydrogen inaccessible to standard RBS due to its low mass.

A variation of RBS with a H^+ ion beam is often called Enhanced Proton Scattering (EPS) due to the nuclear resonance effects which have to be taken into account. Protons can be backscattered by all elements (including deuterium) but this interaction process cannot be described by the Rutherford approximation. Figure 4.3 shows an example of an EPS spectra used for determination of the Be content on a stainless steel mirror holder (*Paper VI*).

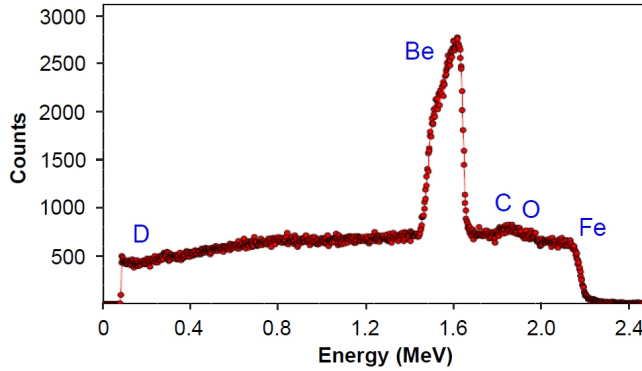


Figure 4.3: EPS studies of a stainless steel mirror holder after exposure in JET. This spectrum was used for determination of the Be content on the holder (*Paper VI*). Proton beam energy is 2.5 MeV.

Nuclear reaction analysis

Nuclear Reaction Analysis (NRA), as it can be seen from the name, utilizes products of a nuclear reaction which occurs between the projectile and the target nucleus. Each nuclear reaction is unique and the emitted radiation is characteristic for that reaction. A broad database of experimental cross-sections for the most used reactions has been created over the last decades [124].

For fuel retention studies, the most important nuclear reaction is the interaction of a ^3He beam with light nuclei in the target: especially D atoms and also ^9Be , ^{12}C , ^{13}C . A standard form to write the ^3He -D reaction is $D(^3\text{He},p)^4\text{He}$, where protons and α -particles are products of the reaction. The corresponding cross-section has a maximum value at beam energy ~ 0.65 MeV, but higher energies allow for greater depth profiles. For a ^3He beam of 2 MeV, protons have an energy of 11.8 MeV and are easily distinguishable on the NRA spectrum. Figure 4.4a shows an example of the NRA spectra for D.

Another example of a NRA spectrum can be seen in Figure 4.4b where a 2.8 MeV ^3He beam was used to investigate the amount of carbon in the deposited thin films. The nuclear reaction $^{12}\text{C}(^3\text{He},p)^{14}\text{N}$ results in three easily distinguishable peaks

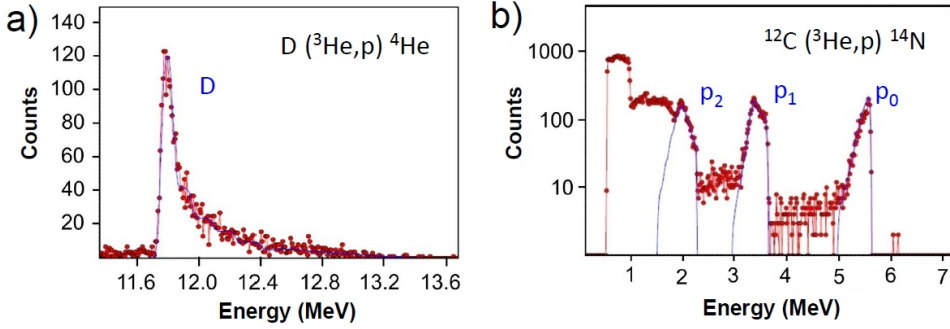


Figure 4.4: a) Deuterium peak of the $D(^3\text{He},p)^4\text{He}$ reaction; b) experimental (red) and SIMNRA simulated (blue) NRA spectra showing a) three carbon peaks of the $^{12}\text{C}(^3\text{He},p)^{14}\text{N}$ reaction marked as p_0 , p_1 and p_2 . The ^3He beam energy is 2.8 MeV for both spectra.

corresponding to the protons of different energies ($p_0 = 5.6$ MeV, $p_1 = 3.62$ MeV, $p_2 = 2.25$ MeV) [125].

Elastic recoil detection analysis

The physical process behind the Elastic Recoil Detection Analysis (ERDA) is the forward-scattering of the recoiling ions. Due to the requirement of low angles of incidence the use of ERDA is restricted to thin surface layers ($< 1\mu\text{m}$) on smooth surfaces. One of the strongest advantages of ERDA is its sensitivity to isotopes. The 2 MeV beams of ^4He are used to measure H and D profiles while employing heavier ions (typically ^{127}I or ^{197}Au) allows to detect other low-Z elements such as ^4He , ^9Be , ^{10}B , ^{11}B , ^{12}C , ^{13}C , ^{14}N , ^{15}N , ^{16}O , ^{18}O , ^{20}Ne [126][127].

ERDA, like RBS, is a quantitative technique and gives exact information about the isotope concentration in the sample. Figure 4.5a shows an ERDA spectrum (36 MeV ^{127}I) registered with a time-of-flight (ToF) detector. In this example the following impurities in the first 100 nm of the surface layer were under investigation: Be ($1.62 \cdot 10^{16}$ at/cm²), C ($1.28 \cdot 10^{16}$ at/cm²), O ($2.91 \cdot 10^{16}$ at/cm²).

Secondary ion mass spectrometry

Secondary Ion Mass Spectrometry (SIMS) is the most sensitive measuring technique capable of detecting $1 \cdot 10^8$ at/cm² [122][128]. Under the continuous bombardment of a target with a 2-10 keV ion beam (e.g. Ar^+ , Cs^+ , O^- , O_2^+ , Ga^+) the target material is removed layer by layer. The sputtered species are emitted as neutrals, ions (both negative and positive) and clusters of particles. The ratio of ionised and neutral species depends on the surface conditions, chemical surroundings and the

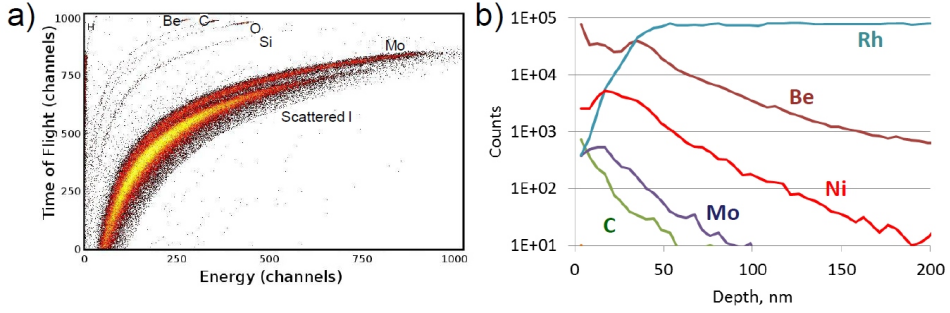


Figure 4.5: a) ToF-ERDA spectrum for a molybdenum mirror after cleaning (*Paper VIII*). Different elements in the sample can be seen as curves in the spectrum; b) example of a SIMS spectra from *Paper VII*

element itself making the quantification challenging. This fact is the main drawback of SIMS when studies of the fusion PFCs are considered.

SIMS is commonly used for detection of low concentrations of impurities and for obtaining depth information on the elemental composition. In *Paper VII* SIMS measurements were performed on the molybdenum and rhodium-coated mirrors after their exposure in JET. These results were decisive for the identification of the qualitative composition in the near-surface layer, i.e. in the region responsible for the change of the mirror reflectivity. One example of a depth profile is demonstrated in Figure 4.5b.

Table 4.1: Summary of the IBA methods relevant for this work.

Method	Studied isotope / Reaction	Beam / Energy	Advantages and limitations
RBS	Li – Pb	$^4\text{He}^+$ / 1.5 – 2.5 MeV	(+)High sensitivity for high-Z elements (-)Poor mass resolution for high-Z elements (-)D detection is not possible
EPS	D / D(p,p)D $^{12}\text{C} / ^{12}\text{C}(\text{p,p})^{12}\text{C}$ $^{13}\text{C} / ^{13}\text{C}(\text{p,p})^{13}\text{C}$	protons / 1.5 – 2.5 MeV protons / ~ 1.75 MeV protons / ~ 1.46 MeV	(+)High selectivity (especially at resonance)
NRA	D / D($^3\text{He,p}$) ^4He $^9\text{Be} / ^9\text{Be}(^3\text{He,p})^{11}\text{B}$ $^{12}\text{C} / ^{12}\text{C}(^3\text{He,p})^{14}\text{N}$	^3He / 0.7 – 3.0 MeV ^3He / ~ 2.5 MeV ^3He / ~ 2.8 MeV	(+)High selectivity (+)Depth profiling for D (-)Ion-induced detrapping of H(D)
ERDA	H, D All elements	$^4\text{He}^+$ / 2 MeV ^{127}I , ^{197}Au / 30 – 200 MeV	(+)High sensitivity for light elements (H,D, He) (+)Easy isotope separation
SIMS	all elements	Ar^+ , Cs^+ , O^- , O_2^+ , Ga^+ / 1 – 30 keV	(+)Good depth profiling ($> 10 \mu\text{m}$) (+)Good depth resolution ($< 100 \text{ nm}$) (+)High sensitivity (-)Poor quantification (-)Destructive (-)Relatively slow

4.4 Gas phase control

Thermal desorption spectrometry

Fuel retention studies require methods to quantify the amount of hydrogen isotopes in PFMs. The previously described techniques give local results but extrapolation of local measurements is not always straightforward due to the non-uniform structure of fuel-rich co-deposits.

Determination of the total fuel content can be performed by Thermal Desorption Spectrometry (TDS) [129]. TDS allows to measure the total amount of desorbed gases from a sample when the latter is placed in a temperature-programmed oven, like the one shown in Figure 3.1. When the material is heated, the energy transferred to the previously adsorbed species will weaken the chemical bonds and cause desorption of volatile components. To quantify the amount of released molecules, a quadrupole mass spectrometer (QMS) is commonly used.

The main principle of a QMS for ion detection is based on the usage of four parallel metal rods placed in a vacuum with a voltage applied to each pair of rods. Ions travelling between the rods are deflected from their original trajectory due to the presence of a magnetic field. For every given voltage value only ions with a certain mass-to-charge ratio (M , also called mass number) will reach the detector. Since only charged particles can be deflected by a quadrupole system, an ioniser should be installed at the quadrupole entrance. Variation of the voltage, applied to the rods, allows to scan over different M (typically in the range 1 – 200) and to observe the mass number distribution at a chosen moment. Repetitive scans will give a time evolution for each type of molecules.

In the TDS setup at FZ Jülich several masses can be measured simultaneously providing the intensity of each mass as a function of temperature and time. The total amount of adsorbed species is given by the integral of the spectrum. In the case of carbon co-deposits, the main interest is associated with masses: $M2$ (H_2), $M3$ (HD), $M4$ (D_2), $M18$ – $M20$, i.e. the water group and various hydrocarbons $C_xH_yD_z$.

Optical spectroscopy

During the laser-induced ablation studies (*Papers II and IV*) a plasma plume during the laser-surface interaction was observed with a commercial spectrometer (Multichannel Instruments: Mechelle 7500), which is also used for boundary plasma studies on TEXTOR. This spectrometer uses two dispersive elements: a grating for dispersion of light in the horizontal plane and a prism to sort orders in the vertical direction. The spectrum is then recoded by an actively cooled CCD. A cross-dispersion setup allows covering the spectral range from 375 to 715 nm.

The light from the plasma plume was directed to the spectrometer through the combination of two lenses and an optical fiber. The produced spectra give additional information on the composition of the ablated matter. Figure 4.6 demonstrates the

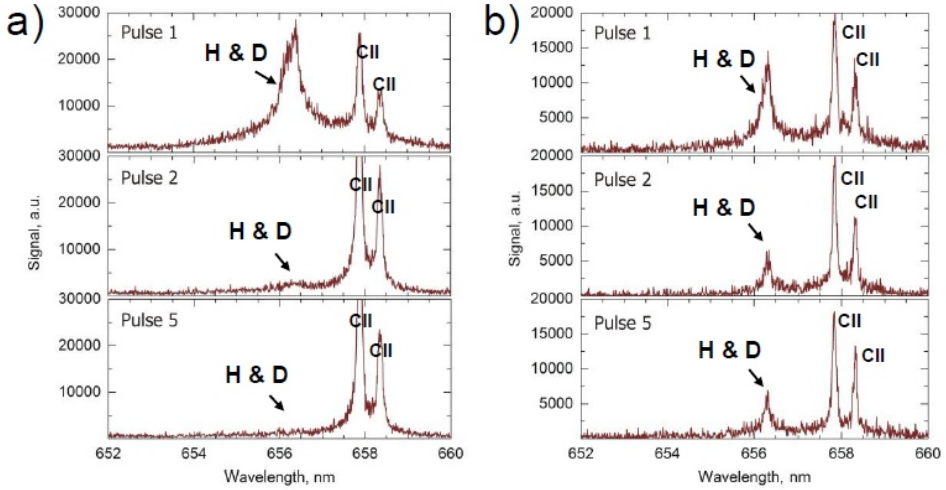


Figure 4.6: Reduction of H (656.3 nm) and D (656.1 nm) line intensities during consecutive laser pulses at a rate 6 pulse/minute. Remaining lines at 657.8 nm and 658.3 nm belong to CII. Spectra are given for ablation of deposits on ALT-II (a) and tungsten coated limiter (b).

spectra recorded during consecutive laser pulses (energy density 14 J/cm^2) on the ALT-II tile with a thick deposit and tungsten coated limiter. It demonstrates effective removal of the layer. To collect species liberated by the ablation, several catchers have been developed and used.

Chapter 5

Impact of PWI on diagnostic components

Mirror, mirror on the wall

Brothers Grimm

5.1 Diagnostic mirrors

ITER will require an extensive system of diagnostics to ensure safe operation and to provide the measurements necessary for fusion research. The major optical diagnostics, e.g. Thomson scattering, will have access to the main vessel through optical labyrinths in the neutron shielding blocks. The first elements in these optical systems will be metallic mirrors also known as *first mirrors* [130][131]. Like all other plasma-facing components, the first mirrors are subject to degradation due to UV and γ radiation, neutron fluxes and impact of neutrals (e.g. charge exchange atoms, hydrocarbons). Depending on their location and the plasma conditions, the mirrors may be in either erosion or deposition dominated areas. The ongoing research at the major fusion experiments, i.e. JET [132], TEXTOR [133][134], DIII-D [135][136], Tore Supra [137], HL-2A [138] is aiming to determine of the modification of mirrors and to elaborate solutions for prolonging their lifetime.

5.2 First Mirror Test at JET

The First Mirror Test (FMT) at JET is an ongoing project which started on the request of the ITER Design Team in 2002. The aim of the project is to examine the optical performance of tested specimens and to elucidate the cause of reflectivity losses. The experiment in JET offers the ITER-relevant combination of plasma configuration and placement of mirrors in critical locations. Locations for the mirror positioning were selected to reproduce in the best achievable way the ITER

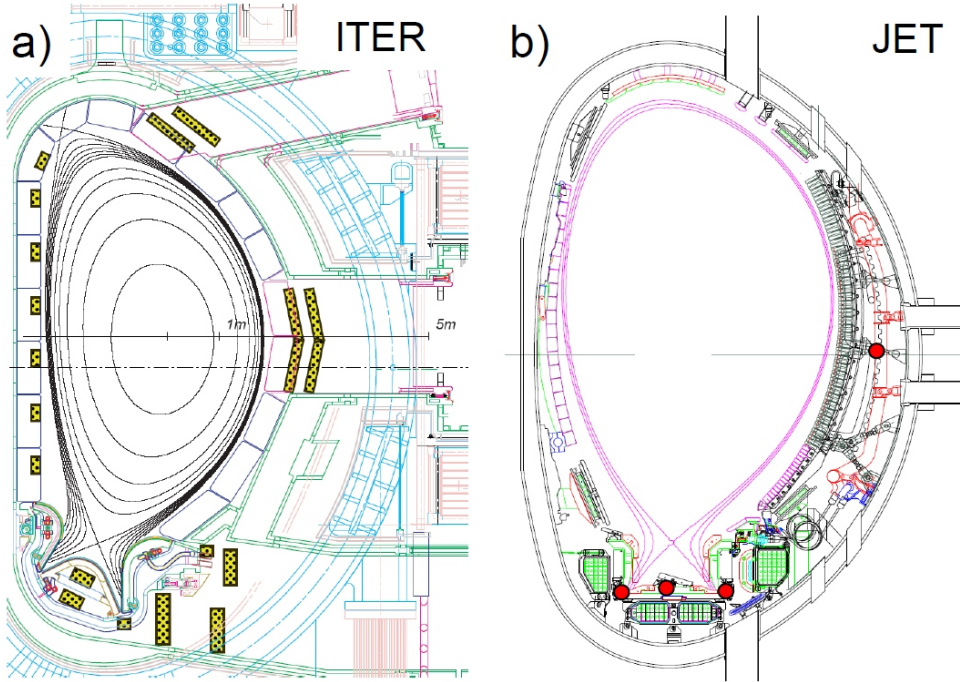


Figure 5.1: Design locations (yellow marking) of the first mirrors in ITER (a) and the location of the test first mirrors in JET (b). [132]

conditions as demonstrated in Figure 5.1. Figure 5.2 shows examples of mirror samples before the exposure and a single cassette for installation of mirrors in the torus.

The entire FMT research program comprises: (a) the selection of the material for the test mirrors, (b) manufacturing of mirrors and their carriers for in-vessel installation, (c) optical pre-characterisation, (d) exposure in the plasma boundary of JET for a complete operational campaign, (e) a broad range of post-exposure analyses by means of optical and surface analysis methods, (f) correlation with erosion deposition pattern measured by other wall diagnostics used in tritium retention studies, (g) cleaning of the exposed mirrors followed by (h) the analyses of cleaned surfaces. The last four points were explored within this thesis (*Papers VI-VIII*).

Two phases of the FMT project were completed in JET with carbon walls: Phase I: 2004-2007 [139], Phase II: 2008-2009 [140]. Over 60 mirror samples made of various materials (stainless steel, molybdenum, rhodium-coated molybdenum [141]) were studied. The mirrors exposed in JET with the ITER-Like Wall (2011-2012) will be retrieved from the vessel in early 2013.

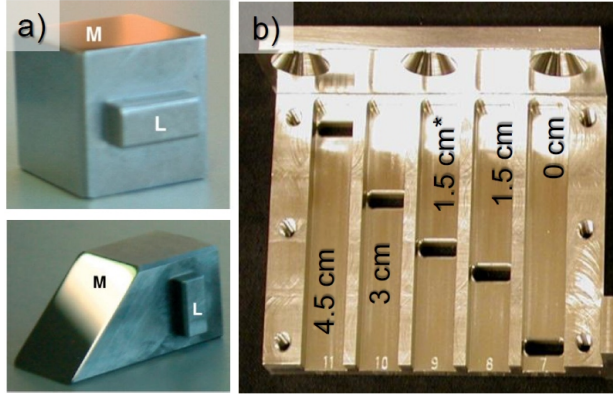


Figure 5.2: a) Flat and angled metallic mirrors as used in FMT. The surface area of a square mirror is 1 cm^2 ; b) the bottom part of a cassette with slits for fixation of mirrors. The indicated distance denotes how far the surface of the mirror is from the channel mouth. The channel marked with “*” is designed for the 45° angled mirrors.

Characterization of mirrors

All materials exposed at JET, and mirrors are no exception here, are contaminated by Be and T and require special precautions during ex-situ studies. The reflectivity measurements were performed directly at JET using an efficient system for total reflectivity determination. It consists of two spectrophotometers (for visible and infrared (IR) light) and an integrating sphere which comes in direct contact with the mirror surface. An identical integrating sphere was used outside of the beryllium-handling facility for studies of the not contaminated samples. The initial calibration of the system was performed using the samples pre-characterized on complex equipment, Varian-Cary 5, at the University of Basel. This calibration is considered sufficient since the main goal is to observe the change of reflectivity.

The optical properties of all mirrors exposed in the divertor were degraded by strong deposition of wall materials such as carbon and beryllium while erosion by plasma impurity species (C, D, Be, Ni, etc) influenced mirrors on the main chamber wall [142]. Implementation of deposition mitigation techniques [135][143] may prolong the mirror lifetime but none of the methods discussed up to date is able to completely eliminate the growth of deposit. Even thin deposited layers (10 nm) can reduce the reflectivity of a mirror due to interference effects [130], while the thickness of deposits after exposure in JET often exceeds the micrometre range. Such effects may be expected in ITER, hence efforts are directed towards development and assessment of procedures for reflectivity recovery.

Cleaning of mirrors

Some techniques for the removal of co-deposits are based on irradiation of PFC with a high-energy scanning laser beam. Photonic methods provide a possibility of remote operation for in-situ applications and demonstrate reliable removal of carbon layers under laboratory conditions [144][145]. However, when tested on the Be-containing deposits from JET, the laser cleaning did not give satisfactory results (*Paper VI*). Despite multiple laser scans with the predefined laser parameters, it was not possible to remove all deposits and at the same time damage to the mirror surface occurred: micro-cracking and local melting. The optimization of laser parameters would be challenging as each type of deposit has a different composition, thickness, density and adherence. This in turn, would require a specific set of parameters for each kind of co-deposit to ensure efficient removal. Alternative cleaning techniques were tested to check whether the removal of complex layers can be efficiently achieved (*Paper VIII*). The results of all cleaning attempts lead to the conclusion that in the case of a carbon surrounding a replacement of the degraded mirrors, though very challenging from the engineering point of view, would probably be the most practical solution.

Chapter 6

Summary

*But then science is nothing but a series of questions
that lead to more questions.*

Sir Terry Pratchett

In this chapter the main outcome of research presented in the thesis is summarised. Systematic qualitative and quantitative studies were carried out in order to determine:

- properties of material migration products, i.e. co-deposited layers and dust particles;
- impact of fuel removal methods on dust generation and on modification of PFCs;
- efficiency of fuel and deposit removal techniques;
- degradation mechanism of diagnostic components - mirrors - and methods of their regeneration.

The study was performed mainly for materials retrieved from tokamaks: special long- and short-term probes and plasma-facing components from TEXTOR, Tore Supra and JET. This has implied research on three major materials used in the technology of the plasma-facing wall: carbon, beryllium and tungsten – a material tested in TEXTOR. The major part of the thesis has dealt with carbon-based components and consequences of their presence for plasma-wall interactions and fuel retention. Such studies are fully justified because carbon is still (December 2012) considered for the ITER divertor and, the large-scale test of the metal wall has just started.

Paper I: Survey of Dust Particles in TEXTOR

The results strongly indicate that in a carbon-wall machine, such as TEXTOR, the disintegration of flaking co-deposits on PFCs is the main source of dust. Their

structure is strongly related to the surface temperature of the PFCs on which flaking co-deposits were formed. The performed estimations indicate a low conversion factor of deposit to dust. For TEXTOR it is about 0.5%. Flaking and detachment of co-deposits is enhanced by the exposure to air.

An important finding is the evidence for the existence of carbon debris, 10 nm – 200 μ m in size, in the collected material. The presence of fine crystalline matter on the bottom of the TEXTOR liner gives some indication that also brittle destruction of carbon tiles could occur. It is the first documented example of brittle destruction products in a tokamak. The study shows that brittle destruction (and dust, in general) is not a serious issue in present-day machines, but it must be taken into account when dust production in future devices in the presence of carbon PFCs is considered.

Papers II and IV: Removal efficiency of fuel and deposits

The efficiency of fuel removal methods has been tested on deuterium-rich carbon co-deposits on limiters from TEXTOR. Systematic experiments aiming at the monitoring of fuel release during long-term annealing (70 h) of deposits at 623 K were carried out for the first time. The aim was to assess the efficiency of fuel removal at the maximum baking temperature of the ITER divertor. The annealing resulted in the release of only 10%-15% of the accumulated deuterium. Very similar results were obtained during long-term annealing of deposits from the Tore Supra tokamak.

Efficient removal of the deposited layer has been achieved by means of laser-induced ablation, but the cleaning procedure has lead to the generation of a large amount of dust. A notable problem is associated with fuel remaining in the ablated products. The observed D/C concentration ratio in the collected products of ablation is about 40% of the initial fuel content in the co-deposits.

Paper IV, which is a follow up of *Paper II*, summarises several fuel removal techniques which were tested during the last decade on PFCs from the TEXTOR tokamak.

Paper III: Re-absorption of fuel

Fuel re-absorption by thermally depleted co-deposited layers was assessed for the first time. The study was performed for a number of probes with co-deposits obtained from TEXTOR limiter tiles. They were outgased at 1273 K and then exposed again to plasma either in a laboratory setup or in TEXTOR. Adsorption of fuel species was identified as the dominant mechanism for deuterium retention in the re-exposed deposits. Fuel retention in the re-exposed deposits is 30–40 times lower than that in the original co-deposit, showing that fuel re-absorption does not lead to an immediate re-saturation of deposits. This can be considered as a very positive results indicating that surfaces cleaned by heating would not re-absorb large amounts of fuel.

Paper V: Wall erosion in JET with carbon PFCs

This work aimed at the reconstruction of a global balance for carbon in JET in the 2007 – 2009 campaign when JET was operating with carbon PFCs. The net deposition of carbon in the divertor and the net erosion in the main chamber were evaluated based on the profilometry of the tiles retrieved from JET. Additionally the spectroscopic measurements of the carbon erosion yield from the main chamber were used for comparison with the profilometry measurements. About 800 grams of carbon was found in the divertor, while the erosion of the material from the main wall is between 400 grams (profilometry data) and 2000 grams (spectroscopy data).

Papers VI, VII and VIII: First Mirror Test

This work was executed in the frame of the First Mirror Test carried out at JET for ITER. A large set of test mirrors was exposed in JET with carbon walls throughout several experimental campaigns. For all mirrors a significant loss of reflectivity was observed following the exposure in a tokamak (*Paper VII*). In order to restore the reflectivity different cleaning techniques, such as laser-induced ablation (*Paper VI*) and mechanical methods (*Paper VIII*), were applied to assess their cleaning efficiency of degraded mirrors.

Laser cleaning lead to partial recovery of the optical performance, however damage (e.g. micro-cracking and local melting) was observed on all laser-cleaned surfaces. The efficiency of laser cleaning depends on the composition of the treated layer. The removal of beryllium-containing deposits was the main challenge. Mechanical removal of deposits (i.e. by polishing) allows for recovery of the initial reflectivity when the cleaning conditions are selected individually for each mirror. The results of all cleaning attempts lead to the conclusion that in the case of the carbon surroundings a replacement of the degraded mirrors would be the most practical solution.

In summary, the research has identified several phenomena accompanying material migration and fuel retention in tokamaks. Various practical aspects of fuel and co-deposit removal techniques have been assessed. In some cases (e.g. first mirrors, laser-induced cleaning), this has also lead to the formulation of recommendations for solutions to be considered in cleaning procedures. The author realizes that certain processes presented in the thesis will be different, both in qualitative and quantitative terms, in controlled fusion devices with metal walls. The work in that direction has begun.

References

- [1] J. Ongena and G. V. Oost, “Energy for future centuries,” *Transactions of Fusion Science and Technology*, vol. 57, no. 2T, pp. 3–15, 2010.
- [2] D. J. MacKay, *Sustainable Energy - Without the Hot Air*. UIT Cambridge Ltd, 2009.
- [3] H. A. Bethe, “Energy production in stars,” *Physical Review*, vol. 55, pp. 103–103, 1939.
- [4] “ITER project.” <http://www.iter.org>.
- [5] J. Wesson, *Tokamaks*. Oxford University Press, 2004.
- [6] M. Abdou, E. Vold, C. Gung, M. Youssef, and K. Shin, “Deuterium–Tritium fuel self-sufficiency in fusion reactors,” *Fusion Technology*, vol. 9, pp. 250–285, 1986.
- [7] L. Giancarli, M. Abdou, D. Campbell, V. Chuyanov, M. Ahn, M. Enoeda, C. Pan, Y. Poitevin, E. R. Kumar, I. Ricipito, Y. Strebkov, S. Suzuki, P. Wong, and M. Zmitko, “Overview of the iter tbm program,” *Fusion Engineering and Design*, in press, 2012.
- [8] J. D. Lawson, “Some criteria for a power producing thermonuclear reactor,” *Proceedings of the Physical Society. Section B*, vol. 70, pp. 6–10, 1957.
- [9] M. Tabak, J. Hammer, M. Glinsky, W. Kruer, S. Wilks, J. Woodworth, E. Campbell, M. Perry, and R. Mason, “Ignition and high gain with ultrapowerful lasers,” *Physics of Plasmas*, vol. 1, no. 5, pp. 1626–1634, 1994.
- [10] S. Atzeni, “Laser driven inertial fusion: the physical basis of current and recently proposed ignition experiments,” *Plasma Physics and Controlled Fusion*, vol. 51, no. 12, p. 124029, 2009.
- [11] J. Lindl, “Progress towards ignition on the National Ignition Facility,” *Nuclear Fusion*, vol. 51, no. 9, 2011.
- [12] “NIF project.” <https://lasers.llnl.gov/>.
- [13] “Laser Mégajoule project.” <http://www-lmj.cea.fr/>.
- [14] F. Romanelli, M. Laxåback, and on behalf of the JET EFDA Contributors, “Overview of JET results,” *Nuclear Fusion*, vol. 51, no. 9, p. 094008, 2011.

- [15] C. Greenfield and the DIII-D Team, “DIII-D contributions towards the scientific basis for sustained burning plasmas,” *Nuclear Fusion*, vol. 51, no. 9, p. 094009, 2011.
- [16] A. Kallenbach and the ASDEX Upgrade Team, “Overview of ASDEX Upgrade results,” *Nuclear Fusion*, vol. 51, no. 7, p. 094012, 2011.
- [17] B. Saoutic and the Tore Supra Team, “Contribution of Tore Supra in preparation of ITER,” *Nuclear Fusion*, vol. 51, no. 9, p. 094014, 2011.
- [18] U. Samm, “TEXTOR: A pioneering device for new concepts in plasma-wall interaction, exhaust, and confinement,” *Fusion Science and Technology*, vol. 47, no. 2, pp. 73–75, 2005.
- [19] A. Isayama and the JT-60 Team, “Overview of JT-60U results towards the resolution of key physics and engineering issues in ITER and JT-60SA,” *Nuclear Fusion*, vol. 51, no. 9, p. 094010, 2011.
- [20] Y. Kamada and the JT-60SA Team, “Plasma regimes and research goals of JT-60SA towards ITER and DEMO,” *Nuclear Fusion*, vol. 51, no. 9, p. 073011, 2011.
- [21] R. Raman and the NSTX Team, “Overview of physics results from NSTX,” *Nuclear Fusion*, vol. 51, no. 9, p. 094011, 2011.
- [22] H. Yamada and the LHD Experiment Group, “Overview of results from the Large Helical Device,” *Nuclear Fusion*, vol. 51, no. 9, p. 094021, 2011.
- [23] L. Wegener, “Status of Wendelstein 7-X construction,” *Fusion Engineering and Design*, vol. 84, no. 2–6, pp. 106–112, 2009.
- [24] O. Neubauer, G. Czymek, B. Giesen, P. Hüttemann, M. Sauer, W. Schalt, and J. Schruoff, “Design features of the tokamak TEXTOR,” *Fusion Science and Technology*, vol. 47, no. 2, pp. 76–76, 2005.
- [25] V. Philipps, A. Pospieszczyk, A. Huber, A. Kirschner, J. Rapp, B. Schweer, P. Wienhold, G. van Oost, G. Sergienko, T. Tanabe, K. Ohya, M. Wada, T. Ohgo, and M. Rubel, “Experiments with tungsten limiters in TEXTOR-94,” *Journal of Nuclear Materials*, vol. 258–263, Part 1, pp. 858–864, 1998.
- [26] A. Pospieszczyk, T. Tanabe, V. Philipps, G. Sergienko, T. Ohgo, K. Kondo, M. Wada, M. Rubel, W. Biel, A. Huber, A. Kirschner, J. Rapp, and N. Noda, “Operation of TEXTOR-94 with tungsten poloidal main limiters,” *Journal of Nuclear Materials*, vol. 290–293, pp. 947–952, 2001.
- [27] J. Cordier, “Preliminary results and lessons learned from upgrading the Tore Supra actively cooled plasma facing components (CIEL project),” *Fusion Engineering and Design*, vol. 66–68, pp. 59–67, 2003.
- [28] B. Pégourié, C. Brosset, E. Tsitrone, A. Beauté, S. Brémond, J. Bucalossi, S. Carpentier, Y. Corre, E. Delchambre, C. Desgranges, P. Devynck, D. Douai, G. Dunand, A. Ekedahl, A. Escarguel, E. Gauthier, J. Gunn, P. Hertout, S.-H. Hong, F. Kazarian, M. Kočan, F. Linez, Y. Marandet, A. Martinez, M. Mayer, O. Meyer, P. Monier-Garbet, P. Moreau, P. Oddon, J.-Y. Pascal, F. Rimini, J. Roth, F. Saint-Laurent,

- F. Samaille, S. Vartanian, C. Arnas, E. Aréou, C. Gil, J. Lasalle, L. Manenc, C. Martin, M. Richou, P. Roubin, and R. Sabot, “Overview of the deuterium inventory campaign in Tore Supra: Operational conditions and particle balance,” *Journal of Nuclear Materials*, vol. 390–391, no. 0, pp. 550–555, 2009.
- [29] G. Matthews, P. Edwards, T. Hirai, M. Kear, A. Lioure, P. Lomas, A. Loving, C. Lungu, H. Maier, P. Mertens, D. Neilson, R. Neu, J. Pamela, V. Philipps, G. Piazza, V. Riccardo, M. Rubel, C. Ruset, E. Villedieu, and M. Way, “Overview of the ITER-like wall project,” *Physica Scripta*, no. T128, pp. 137–143, 2007.
- [30] G. Matthews, M. Beurskens, S. Brezinsek, M. Groth, E. Joffrin, A. Loving, M. Kear, M.-L. Mayoral, R. Neu, P. Prior, V. Riccardo, F. Rimini, M. Rubel, G. Sips, E. Villedieu, P. de Vries, and M. Watkins, “JET ITER-Like Wall — overview and experimental programme,” *Physica Scripta*, no. T145, p. 014001, 2011.
- [31] G. Federici, C. Skinner, J. Brooks, J. Coad, C. Grisolia, A. Haasz, A. Hassanein, V. Philipps, C. Pitcher, J. Roth, W. Wampler, and D. Whyte, “Plasma-material interactions in current tokamaks and their implications for next step fusion reactors,” *Nuclear Fusion*, vol. 41, pp. 1967–2137, 2001.
- [32] W. Hofer, J. Roth, O. Auciello, and D. Flamm, *Physical Processes of the Interaction of Fusion Plasmas with Solids (Plasma-Materials Interactions)*. Academic Press, 1996.
- [33] A. Loarte, B. Lipschultz, A. Kukushkin, G. Matthews, P. Stangeby, N. Asakura, G. Counsell, G. Federici, A. Kallenbach, K. Krieger, A. Mahdavi, V. Philipps, D. Reiter, J. Roth, J. Strachan, D. Whyte, R. Doerner, T. Eich, W. Fundamenski, A. Herrmann, M. Fenstermacher, P. Ghendrih, M. Groth, A. Kirschner, S. Konoshima, B. LaBombard, P. Lang, A. Leonard, P. Monier-Garbet, R. Neu, H. Pacher, B. Pégourié, R. Pitts, S. Takamura, J. Terry, and E. Tsitrone, “ITER physics basis. Chapter 4: Power and particle control,” *Nuclear Fusion*, vol. 47, no. 6, pp. S203–S263, 2007.
- [34] J. Coad, N. Bekris, J. Elder, S. Erents, D. Hole, K. Lawson, G. Matthews, R.-D. Penzhorn, and P. Stangeby, “Erosion/deposition issues at JET,” *Journal of Nuclear Materials*, vol. 290–293, pp. 224–230, 2001.
- [35] K. Dippel and the TEXTOR Team, “Plasma-wall interaction and plasma performance in TEXTOR — a review,” *Journal of Nuclear Materials*, vol. 145–147, pp. 3–14, 1987.
- [36] A. Kirschner, V. Philipps, M. Rubel, and P. Mertens, “Overview of erosion mechanisms, impurity transport, and deposition in TEXTOR and related modeling,” *Fusion Science and Technology*, vol. 47, no. 2, pp. 146–160, 2005.
- [37] M. Mayer, V. Rohde, J. Likonen, E. Vainonen-Ahlgren, K. Krieger, X. Gong, and J. Chen, “Carbon erosion and deposition on the ASDEX Upgrade divertor tiles,” *Journal of Nuclear Materials*, vol. 337–339, pp. 119–123, 2005.
- [38] A. Kreter, M. J. Balden, R. P. Doerner, D. Nishijima, P. Petersson, A. Pospieszczyk, M. Rubel, and K. Umstadter, “Fuel retention in carbon materials under ITER-relevant mixed species plasma conditions,” *Physica Scripta*, vol. T138, p. 014012, 2009.

- [39] A. Schmidt, I. Uytendhouwen, W. Kühnlein, M. Rödiger, J. Linke, T. Hirai, and G. Pintsuk, “A tritium diagnostic and trap for JUDITH — First results in disruption simulation experiments with neutron irradiated beryllium during cyclic electron beam testing,” *Fusion Engineering and Design*, vol. 83, no. 7—9, pp. 1108–1113, 2008.
- [40] K. Bystrov, J. Westerhout, M. Matveeva, A. Litnovsky, L. Marot, E. Zoethout, and G. De Temmerman, “Erosion yields of carbon under various plasma conditions in Pilot-PSI,” *Journal of Nuclear Materials*, vol. 415, no. 1, Supplement, pp. S149–S152, 2011.
- [41] J. Rapp, W. Koppers, H. van Eck, G. van Rooij, W. Goedheer, B. de Groot, R. Al, M. Graswinckel, M. van den Berg, O. Kruijdt, P. Smeets, H. van der Meiden, W. Vijvers, J. Scholten, M. van de Pol, S. Brons, W. Melissen, T. van der Grift, R. Koch, B. Schweer, U. Samm, V. Philipps, R. Engeln, D. Schram, N. L. Cardozo, and A. Kleyn, “Construction of the plasma-wall experiment Magnum-PSI,” *Fusion Engineering and Design*, vol. 85, no. 7—9, pp. 1455–1459, 2010.
- [42] H. Bolt, V. Barabash, G. Federici, J. Linke, A. Loarte, J. Roth, and K. Sato, “Plasma facing and high heat flux materials – needs for ITER and beyond,” *Journal of Nuclear Materials*, vol. 307–311, Part 1, pp. 43–52, 2002.
- [43] M. Merola, D. Loesser, A. Martin, P. Chappuis, R. Mitteau, V. Komarov, R. Pitts, S. Gicquel, V. Barabash, L. Giancarli, J. Palmer, M. Nakahira, A. Loarte, D. Campbell, R. Eaton, A. Kukushkin, M. Sugihara, F. Zhang, C. Kim, R. Raffray, L. Ferland, D. Yao, S. Sadakov, A. Furmanek, V. Rozov, T. Hirai, F. Escourbiac, T. Jokinen, B. Calcagno, and S. Mori, “ITER plasma-facing components,” *Fusion Engineering and Design*, vol. 85, no. 10—12, pp. 2312–2322, 2010.
- [44] R. Pitts, S. Carpentier, F. Escourbiac, T. Hirai, V. Komarov, A. Kukushkin, S. Lisgo, A. Loarte, M. Merola, R. Mitteau, A. Raffray, M. Shimada, and P. Stangeby, “Physics basis and design of the ITER plasma-facing components,” *Journal of Nuclear Materials*, vol. 415, no. 1, Supplement, pp. S957–S964, 2011.
- [45] M. Shimada, R. Pitts, A. Loarte, D. Campbell, M. Sugihara, V. Mukhovatov, A. Kukushkin, and V. Chuyanov, “ITER research plan of plasma-wall interaction,” *Journal of Nuclear Materials*, vol. 390—391, pp. 282–285, 2009.
- [46] R. Pitts, “A full tungsten divertor for ITER: physics issues and design status,” *Journal of Nuclear Materials*, in press, 2012.
- [47] J. Linke, “High heat flux performance of plasma facing materials and components under service conditions in future fusion reactors,” *Transactions of Fusion Science and Technology*, vol. 57, no. 2T, pp. 293–302, 2010.
- [48] R. Mitteau, P. Stangeby, C. Lowry, and M. Merola, “Heat loads and shape design of the ITER first wall,” *Fusion Engineering and Design*, vol. 85, no. 10—12, pp. 2049–2053, 2010.
- [49] M. Gilbert and J. Sublet, “Neutron-induced transmutation effects in W and W-alloys in a fusion environment,” *Nuclear Fusion*, vol. 51, no. 4, p. 043005, 2011.

- [50] D. Naujoks and R. Behrisch, "Erosion and redeposition at the vessel walls in fusion devices," *Journal of Nuclear Materials*, vol. 220—222, pp. 227–230, 1995.
- [51] V. Philipps, P. Wienhold, A. Kirschner, and M. Rubel, "Erosion and redeposition of wall material in controlled fusion devices," *Vacuum*, vol. 67, no. 3—4, pp. 399–408, 2002.
- [52] R. Pitts, J. Coad, D. Coster, G. Federici, W. Fundamenski, J. Horacek, K. Krieger, A. Kukushkin, J. Likonen, G. Matthews, M. Rubel, and J. Strachan, "Material erosion and migration in tokamaks," *Plasma Physics and Controlled Fusion*, vol. 47, no. 12B, p. B303, 2005.
- [53] R. Behrisch and W. Eckstein, *Sputtering by Particle Bombardment*. Springer, Berlin, 2007.
- [54] P. Sigmund, "Collision theory of displacement damage, ion ranges, and sputtering," *Revue Roumaine de Physique*, vol. 17, no. 7, pp. 823–870, 1972.
- [55] P. Blackburn, M. Hoch, and H. Johnston, "The vaporization of molybdenum and tungsten oxides," *The Journal of Physical Chemistry*, vol. 62, no. 7, pp. 769–773, 1958.
- [56] M. Rubel, G. Sergienko, A. Kreter, A. Pospieszczyk, M. Psoda, and E. Wessel, "An overview of fuel retention and morphology in a castellated tungsten limiter," *Fusion Engineering and Design*, vol. 83, no. 7–9, pp. 1049–1053, 2008.
- [57] J. Linke, S. Amouroux, E. Berthe, Y. Koza, W. Kühnlein, and M. Rödiger, "Brittle destruction of carbon-based materials in transient heat load tests," *Fusion Engineering and Design*, vol. 66–68, pp. 395–399, 2003.
- [58] M. Rubel, P. Wienhold, and D. Hildebrandt, "Fuel accumulation in co-deposited layers on plasma facing components," *Journal of Nuclear Materials*, vol. 290–293, pp. 473–477, 2001.
- [59] C. Linsmeier, J. Luthin, and P. Goldstraß, "Mixed material formation and erosion," *Journal of Nuclear Materials*, vol. 290–293, pp. 25–32, 2001.
- [60] M. Psoda, M. Rubel, G. Sergienko, P. Sundelin, and A. Pospieszczyk, "Material mixing on plasma-facing components: Compound formation," *Journal of Nuclear Materials*, vol. 386–388, pp. 740–743, 2009.
- [61] B. Mills, D. Buchenauer, A. Pontau, and M. Ulrickson, "Characterization of deposition and erosion of the TFTR bumper limiter and wall," *Journal of Nuclear Materials*, vol. 162–164, pp. 343 – 349, 1989.
- [62] R. Doerner, "The implications of mixed-material plasma-facing surfaces in ITER," *Journal of Nuclear Materials*, vol. 363–365, pp. 32–40, 2007.
- [63] G. Matthews, "Plasma operation with metallic walls: direct comparison with the all carbon environment," *Journal of Nuclear Materials*, *in press*, 2012.
- [64] S. Brezinsek, S. Jachmich, M. Stamp, A. Meigs, J. Coenen, K. Krieger, C. Giroud, M. Groth, V. Philipps, R. S. S. Grünhagen, G. van Rooij, D. Ivanova, and G. Matthews, "Residual carbon content in the initial ITER-Like Wall experiments at JET," *Journal of Nuclear Materials*, *in press*, 2012.

- [65] K. Krieger, S. Brezinsek, M. Reinelt, S. Lisgo, J. Coenen, S. Jachmich, S. Marsen, A. Meigs, G. van Rooij, M. Stamp, O. van Hoey, D. Ivanova, T. Loarer, and V. Philipps, "Beryllium migration and evolution of first wall surface composition in the JET ILW configuration," *Journal of Nuclear Materials*, in press, 2012.
- [66] J. Sharpe, D. Petti, and H.-W. Bartels, "A review of dust in fusion devices: Implications for safety and operational performance," *Fusion Engineering and Design*, vol. 63–64, pp. 153–163, 2002.
- [67] J. Winter, "Dust in fusion devices - experimental evidence, possible sources and consequences," *Plasma Physics and Controlled Fusion*, vol. 40, no. 6, pp. 1201–1210, 1998.
- [68] M. Rubel, M. Cecconello, J. Malmberg, G. Sergienko, W. Biel, J. Drake, A. Hedqvist, A. Huber, and V. Philipps, "Dust particles in controlled fusion devices: morphology, observations in the plasma and influence on the plasma performance," *Nuclear Fusion*, vol. 41, pp. 1087–1099, 2001.
- [69] G. McCracken, "A review of the experimental evidence for arcing and sputtering in tokamaks," *Journal of Nuclear Materials*, vol. 93–94, Part 1, pp. 3–16, 1980.
- [70] M. Laux, W. Schneider, B. Jüttner, S. Lindig, M. Mayer, M. Balden, I. Beilis, and B. Djakov, "Modification of tungsten layers by arcing," *Journal of Nuclear Materials*, vol. 337–339, no. 0, pp. 1019–1023, 2005.
- [71] V. Rohde, M. Balden, and T. Lunt, "Dust investigations at ASDEX Upgrade," *Physica Scripta*, vol. T138, p. 014024, 2009.
- [72] J. Linke, M. Rubel, J. Malmberg, J. Drake, R. Duwe, H. Penkalla, M. Rödiger, and E. Wessel, "Carbon particles emission, brittle destruction and co-deposit formation: experience from electron beam experiments and controlled fusion devices," *Physica Scripta*, vol. 2001, no. T91, pp. 36–42, 2001.
- [73] G. Sergienko, B. Bazylev, T. Hirai, A. Huber, A. Kreter, P. Mertens, A. Nedospasov, V. Philipps, A. Pospieszczyk, M. Rubel, U. Samm, B. Schweer, P. Sundelin, M. Tokar, and E. Wessel, "Experience with bulk tungsten test-limiters under high heat loads: melting and melt layer propagation," *Physica Scripta*, vol. 2007, no. T128, p. 81, 2007.
- [74] P. Chappuis, E. Tsitrone, M. Mayne, X. Armand, H. Linke, H. Bolt, D. Petti, and J. Sharpe, "Dust characterization and analysis in Tore-Supra," *Journal of Nuclear Materials*, vol. 290–293, pp. 245–249, 2001.
- [75] Y. Gotoh, T. Tanabe, Y. Ishimoto, K. Masaki, T. Arai, H. Kubo, K. Tsuzuki, and N. Miya, "Long-term erosion and re-deposition of carbon in the divertor region of JT-60U," *Journal of Nuclear Materials*, vol. 357, no. 1–3, pp. 138–146, 2006.
- [76] J. Roth, E. Tsitrone, A. Loarte, T. Loarer, G. Counsell, R. Neu, V. Philipps, S. Brezinsek, M. Lehnen, P. Coad, C. Grisolia, K. Schmid, K. Krieger, A. Kallenbach, B. Lipschultz, R. Doerner, R. Causey, V. Alimov, W. Shu, O. Ogorodnikova, A. Kirschner, G. Federici, and A. Kukushkin, "Recent analysis of key plasma wall interactions issues for iter," *Journal of Nuclear Materials*, vol. 390–391, pp. 1–9, 2009.

- [77] C. Grisolia, S. Rosanvallon, A. Loarte, P. Sharpe, and C. Arnas, "From eroded material to dust: An experimental evaluation of the mobilised dust production in Tore Supra," *Journal of Nuclear Materials*, vol. 390–391, pp. 53–56, 2009.
- [78] R. Causey, "Hydrogen isotope retention and recycling in fusion reactor plasma-facing components," *Journal of Nuclear Materials*, vol. 300, pp. 91–117, 2002.
- [79] G. Counsell, P. Coad, C. Grisolia, C. Hopf, W. Jacob, A. Kirschner, A. Kreter, K. Krieger, J. Likonen, V. Philipps, J. Roth, M. Rubel, E. Salancon, A. Semerok, F. Tabares, and A. Widdowson, "Tritium retention in next step devices and the requirements for mitigation and removal techniques," *Plasma Physics and Controlled Fusion*, vol. 48, no. 12B, pp. B189–B199, 2006.
- [80] D. Stork, *Technical Aspects of Deuterium - Tritium Experiments at JET*. Fusion engineering and design, 1999.
- [81] M. Keilhacker, "Fusion physics progress on JET," *Fusion Engineering and Design*, vol. 46, no. 2–4, pp. 273–290, 1999.
- [82] J. Roth, E. Tsitrone, T. Loarer, V. Philipps, S. Brezinsek, A. Loarte, G. Counsell, R. Doerner, K. Schmid, O. Ogorodnikova, and R. Causey, "Tritium inventory in ITER plasma-facing materials and tritium removal procedures," *Plasma Physics and Controlled Fusion*, vol. 50, no. 10, p. 103001, 2008.
- [83] T. Loarer, C. Brosset, J. Bucalossi, P. Coad, G. Esser, J. Hogan, J. Likonen, M. Mayer, P. Morgan, V. Philipps, V. Rohde, J. Roth, M. Rubel, E. Tsitrone, and A. Widdowson, "Gas balance and fuel retention in fusion devices," *Nuclear Fusion*, vol. 47, no. 9, pp. 1112–1120, 2007.
- [84] M. Mayer, V. Philipps, P. Wienhold, H. Esser, J. von Seggern, and M. Rubel, "Hydrogen inventories in nuclear fusion devices," *Journal of Nuclear Materials*, vol. 290–293, no. 0, pp. 381–388, 2001.
- [85] V. Rohde, M. Mayer, V. Mertens, R. Neu, and K. Sugiyama, "Dynamic and static deuterium inventory in ASDEX Upgrade with tungsten first wall," *Nuclear Fusion*, vol. 49, no. 8, p. 085031, 2009.
- [86] V. Alimov and J. Roth, "Hydrogen isotope retention in plasma-facing materials: review of recent experimental results," *Physica Scripta*, vol. T128, pp. 6–13, 2007.
- [87] L. Leblanc and G. Ross, "Ranges and variances of 0.2–1.0 keV hydrogen and deuterium ions implanted into Be, C and Si," *Nuclear Instruments and Methods in Physics Research Section B*, vol. 83, no. 1–2, pp. 15–20, 1993.
- [88] W. Wampler, D. Brice, and C. Magee, "Saturation of deuterium retention in carbon a new calibration for plasma edge probes," *Journal of Nuclear Materials*, vol. 102, no. 3, pp. 304–312, 1981.
- [89] G. Counsell and C. Wu, "In-situ detection and removal of carbon debris – a challenge for the next-step fusion device," *Physica Scripta*, vol. T91, pp. 70–75, 2001.
- [90] C. Grisolia, G. Counsell, G. Dinescu, A. Semerok, N. Bekris, P. Coad, C. Hopf, J. Roth, M. Rubel, A. Widdowson, and E. Tsitrone, "Treatment of ITER plasma

- facing components: Current status and remaining open issues before ITER implementation,” *Fusion Engineering and Design*, vol. 82, no. 15–24, pp. 2390–2398, 2007.
- [91] R. Causey, W. Wampler, and D. Walsh, “Comparison of the thermal stability of the codeposited carbon/hydrogen layer to that of the saturated implant layer,” *Journal of Nuclear Materials*, vol. 176–177, pp. 987–991, 1990.
 - [92] R. Pitts, A. Kukushkin, A. Loarte, A. Martin, M. Merola, C. Kessel, V. Komarov, and M. Shimada, “Status and physics basis of the ITER divertor,” *Physica Scripta*, vol. T138, p. 014001, 2009.
 - [93] M. Shimada and R. A. Pitts, “Wall conditioning on ITER,” *Journal of Nuclear Materials*, vol. 415, no. 1, Supplement, pp. S1013–S1016, 2011.
 - [94] K. Sugiyama, J. Roth, A. Anghel, C. Porosnicu, M. Baldwin, R. Doerner, K. Krieger, and C. Lungu, “Consequences of deuterium retention and release from Be-containing mixed materials for ITER Tritium Inventory Control,” *Journal of Nuclear Materials*, vol. 415, no. 1, Supplement, pp. S731–S734, 2011.
 - [95] J. F. Ready, *Industrial Applications of Lasers*. Academic Press, 1997.
 - [96] E. Tanzi, J. Lupton, and T. Alster, “Lasers in dermatology: Four decades of progress,” *Journal of the American Academy of Dermatology*, vol. 49, no. 1, pp. 1–34, 2003.
 - [97] K.-J. Halbhauer and K. König, “Modern laser scanning microscopy in biology, biotechnology and medicine,” *Annals of Anatomy*, vol. 185, no. 1, pp. 1–20, 2003.
 - [98] J. Asmus, “Light cleaning: laser technology for surface preparation in the arts,” *Technology and Conservation*, vol. 3, pp. 14–18, 1978.
 - [99] J. Davis, A. Haasz, and P. Stangeby, “Laser induced release of gases from first wall coatings for fusion applications,” *Journal of Nuclear Materials*, vol. 138, no. 2–3, pp. 227–234, 1986.
 - [100] B. Schweer, A. Huber, G. Sergienko, V. Philipps, F. Irrek, H. Esser, U. Samm, M. Kempenaars, M. Stamp, C. Gowers, and D. Richards, “Laser desorption of deuterium retained in re-deposited carbon layers at TEXTOR and JET,” *Journal of Nuclear Materials*, vol. 337–339, pp. 570–574, 2005.
 - [101] P. Gąsior, F. Irrek, P. Petersson, H. Penkalla, M. Rubel, B. Schweer, P. Sundelin, E. Wessel, J. Linke, V. Philipps, B. Emmoth, J. Wolowski, and T. Hirai, “Laser-induced removal of co-deposits from graphitic plasma-facing components: Characterization of irradiated surfaces and dust particles,” *Journal of Nuclear Materials*, vol. 390–391, pp. 585–588, 2009.
 - [102] C. Hernandez, H. Roche, C. Pocheau, C. Grisolia, L. Gargiulo, A. Semerok, A. Varty, P. Delaporte, and L. Mercadier, “Development of a Laser Ablation System Kit (LASK) for tokamak in vessel tritium and dust inventory control,” *Fusion Engineering and Design*, vol. 84, no. 2–6, pp. 939–942, 2009.
 - [103] H. Roche, P. Delaporte, C. Grisolia, P. Languille, T. Loarer, J.-Y. Pascal, B. Pégourié, and E. Tsitrone, “Layer removal in gaps by laser process,” *Journal of Nuclear Materials*, in press, 2012.

- [104] J. Davis and A. Haasz, "Oxidation of carbon deposits as a fuel removal technique for application in fusion devices," *Journal of Nuclear Materials*, vol. 390–391, pp. 532–537, 2009.
- [105] C. Tsui, A. Haasz, J. Davis, J. Coad, and J. Likonen, "Deuterium removal during thermo-oxidation of Be-containing codeposits from JET divertor tiles," *Nuclear Fusion*, vol. 48, no. 3, p. 035008, 2008.
- [106] A. Haasz, J. Likonen, J. Coad, C. Tsui, J. Davis, and A. Widdowson, "Thermo-oxidation and analysis of JET codeposits," *Journal of Nuclear Materials*, vol. 390–391, pp. 626–630, 2009.
- [107] C. Hopf, V. Rohde, W. Jacob, A. Herrmann, R. Neu, and J. Roth, "Oxygen glow discharge cleaning in ASDEX Upgrade," *Journal of Nuclear Materials*, vol. 363–365, pp. 882–887, 2007.
- [108] M. Rubel, G. De Temmerman, G. Sergienko, P. Sundelin, B. Emmoth, and V. Philipps, "Fuel removal from plasma-facing components by oxidation-based techniques. an overview of surface conditions after oxidation," *Journal of Nuclear Materials*, vol. 363–365, pp. 877–881, 2007.
- [109] P. Wang, W. Jacob, M. Balden, A. Manhard, and T. Schwarz-Selinger, "Erosion of tungsten-doped amorphous carbon films in oxygen plasma," *Journal of Nuclear Materials*, vol. 420, no. 1–3, pp. 101–109, 2012.
- [110] V. Philipps, G. Sergienko, A. Lyssoivan, H. Esser, M. Freisinger, A. Kreter, and U. Samm, "Removal of carbon layers by oxygen glow discharges in TEXTOR," *Journal of Nuclear Materials*, vol. 363–365, no. 0, pp. 929–932, 2007.
- [111] F. Tabarés, D. Tafalla, V. Rohde, M. Stamp, G. Matthews, G. Esser, V. Philipps, R. Doerner, and M. Baldwin, "Studies of a-C: D film inhibition by nitrogen injection in laboratory plasmas and divertors," *Journal of Nuclear Materials*, vol. 337–339, no. 0, pp. 867–871, 2005.
- [112] P. Sundelin, C. Schulz, V. Philipps, M. Rubel, G. Sergienko, and L. Marot, "Nitrogen-assisted removal of deuterated carbon layers," *Journal of Nuclear Materials*, vol. 390–391, pp. 647–650, 2009.
- [113] F. Tabarés, J. Ferreira, A. Ramos, D. Alegre, G. van Rooij, J. Westerhout, R. Al, J. Rapp, A. Drenik, and M. Mozetic, "Tritium control techniques in ITER by ammonia injection," *Journal of Nuclear Materials*, vol. 415, no. 1, Supplement, pp. S793–S796, 2011.
- [114] D. Douai, A. Lyssoivan, V. Philipps, V. Rohde, T. Wauters, T. Blackman, V. Bobkov, S. Brémond, S. Brezinsek, F. Clairet, E. de la Cal, T. Coyne, E. Gauthier, T. Gerbaud, M. Graham, S. Jachmich, E. Joffrin, R. Koch, A. Kreter, R. Laengner, P. Lamalle, E. Lerche, G. Lombard, M. Maslov, M.-L. Mayoral, A. Miller, I. Monakhov, J.-M. Noterdaeme, J. Ongena, M. Paul, B. Pégourié, R. Pitts, V. Plyusnin, F. Schüller, G. Sergienko, M. Shimada, A. Sirinelli, W. Suttrop, C. Sozzi, M. Tsalas, E. Tsitrone, B. Unterberg, and D. V. Eester, "Recent results on Ion Cyclotron Wall Conditioning in mid and large size tokamaks," *Journal of Nuclear Materials*, vol. 415, no. 1, Supplement, pp. S1021–S1028, 2011.

- [115] T. Wauters, “Hydrogen Ion Cyclotron Wall Conditioning for fuel removal on TEXTOR and ASDEX Upgrade,” *EPS-2012, P4.086*, 2012.
- [116] D. Ivanova, P. Petersson, M. Rubel, A. Kreter, S. Möller, V. Philipps, M. Freisinger, and T. Wauters, “Impact of thermal treatment and ICWC on fuel inventory in co-deposits,” *EPS-2012, P1.054*, 2012.
- [117] J. Mayer and E. Rimini, *Ion Beam Handbook for Material Analysis*. Academic Press, 1977.
- [118] J. Tesmer, M. Nastasi, J. Barbour, C. Maggiore, and J. Mayer, *Handbook of Modern Ion Beam Materials Analysis*. Materials Research Society, Pittsburgh, PA, 1995.
- [119] R. Behrisch, “Measurement of hydrogen isotopes in plasma-facing materials of fusion devices,” *Physica Scripta*, vol. 2001, no. T94, p. 52, 2001.
- [120] M. Rubel, P. Wienhold, and D. Hildebrandt, “Ion beam analysis methods in the studies of plasma facing materials in controlled fusion devices,” *Vacuum*, vol. 70, no. 2—3, pp. 423 – 428, 2003.
- [121] W. Wampler, “Ion beam analysis for fusion energy research,” *Nuclear Instruments and Methods in Physics Research Section B: Beam Interactions with Materials and Atoms*, vol. 219—220, pp. 836–845, 2004.
- [122] M. Rubel, “Analysis of plasma facing materials: material migration and fuel retention,” *Physica Scripta*, vol. T123, pp. 54–65, 2006.
- [123] P. Petersson, *Ion beam analysis of first wall materials exposed to plasma in controlled thermonuclear fusion devices*. Doctoral Thesis, Uppsala University, 2010.
- [124] “Online database of nuclear reactions.” <http://www-nds.iaea.org/iband1/>.
- [125] H.-M. Kuan, T. Bonner, and J. Risser, “An investigation of the C12 + He3 reactions at bombarding energies between 1.8 and 5.4 MeV,” *Nuclear Physics*, vol. 51, pp. 481–517, 1964.
- [126] U. Kreissig, R. Grötzschel, and R. Behrisch, “Simultaneous measurement of the hydrogen isotopes H, D, T and 3He with HIERD,” *Nuclear Instruments and Methods in Physics Research Section B: Beam Interactions with Materials and Atoms*, vol. 85, no. 1—4, pp. 71–74, 1994.
- [127] P. Petersson, M. Rubel, G. Possnert, S. Brezinsek, and B. Pégourié, “Nuclear reaction and heavy ion ERD analysis of wall materials from controlled fusion devices: Deuterium and Nitrogen-15 studies,” *Nuclear Instruments and Methods in Physics Research Section B: Beam Interactions with Materials and Atoms*, vol. 273, pp. 113–117, 2012.
- [128] A. Benninghoven, “Surface analysis by Secondary Ion Mass Spectrometry (SIMS),” *Surface Science*, vol. 299–300, pp. 246–260, 1994.
- [129] P. Redhead, “Thermal desorption of gases,” *Vacuum*, vol. 12, pp. 203–211, 1962.
- [130] A. Costley, T. Sugie, G. Vayakis, and C. Walker, “Technological challenges of ITER diagnostics,” *Fusion Engineering and Design*, vol. 74, no. 1—4, pp. 109–119, 2005.

- [131] V. Voitsenya, A. Bardamid, V. Bondarenko, W. Jacob, V. Konovalov, S. Masuzaki, O. Motojima, D. Orlinskij, V. Poperenko, I. Ryzhkov, A. Sagara, A. Shtan, S. Solodovchenko, and M. Vinnichenko, "Some problems arising due to plasma-surface interaction for operation of the in-vessel mirrors in a fusion reactor," *Journal of Nuclear Materials*, vol. 290–293, pp. 336–340, 2001.
- [132] M. Rubel, G. De Temmerman, J. Coad, J. Vince, J. Drake, a. A. M. F. Le Guern, R. Pitts, and C. Walker, "Analysis of plasma facing materials: material migration and fuel retention," *Review of Scientific Instruments*, vol. 77, no. 6, p. 063501, 2006.
- [133] P. Wienhold, A. Litnovsky, V. Philipps, B. Schweer, G. Sergienko, P. Oelhafen, M. Ley, G. De Temmerman, W. Schneider, D. Hildebrandt, M. Laux, M. Rubel, and B. Emmoth, "Exposure of metal mirrors in the scrape-off layer of TEXTOR," *Journal of Nuclear Materials*, vol. 337–339, pp. 1116–1120, 2005.
- [134] A. Litnovsky, P. Wienhold, V. Philipps, G. Sergienko, O. Schmitz, A. Kirschner, A. Kreter, S. Droste, U. Samm, P. Mertens, A. Donné, D. Rudakov, S. Allen, R. Boivin, A. McLean, P. Stangeby, W. West, C. Wong, M. Lipa, B. Schunke, G. D. Temmerman, R. Pitts, A. Costley, V. Voitsenya, K. Vukolov, P. Oelhafen, M. Rubel, and A. Romanyuk, "Diagnostic mirrors for ITER: A material choice and the impact of erosion and deposition on their performance," *Journal of Nuclear Materials*, vol. 363–365, pp. 1395–1402, 2007.
- [135] D. Rudakov, J. Boedo, R. Moyer, A. Litnovsky, V. Philipps, P. Wienhold, S. Allen, M. Fenstermacher, M. Groth, C. Lasnier, R. Boivin, N. Brooks, A. Leonard, W. West, C. Wong, A. McLean, P. Stangeby, G. De Temmerman, W. Wampler, and J. Watkins, "First tests of molybdenum mirrors for ITER diagnostics in DIII-D divertor," *Review of Scientific Instruments*, vol. 77, no. 10, p. 10F126, 2006.
- [136] A. Litnovsky, D. Rudakov, G. De Temmerman, P. Wienhold, V. Philipps, U. Samm, A. McLean, W. West, C. Wong, N. Brooks, J. Watkins, W. Wampler, P. Stangeby, J. Boedo, R. Moyer, S. Allen, M. Fenstermacher, M. Groth, C. Lasnier, R. Boivin, A. Leonard, A. Romanyuk, T. Hirai, G. Pintsuk, U. Breuer, and A. Scholl, "First tests of diagnostic mirrors in a tokamak divertor: An overview of experiments in DIII-D," *Fusion Engineering and Design*, vol. 83, no. 1, pp. 79–89, 2008.
- [137] M. Lipa, B. Schunke, C. Gil, J. Bucalossi, V. Voitsenya, V. Konovalov, K. Vukolov, M. Balden, G. De Temmerman, P. Oelhafen, A. Litnovsky, and P. Wienhold, "Analyses of metallic first mirror samples after long term plasma exposure in Tore Supra," *Fusion Engineering and Design*, vol. 81, no. 1–7, pp. 221–225, 2006.
- [138] Y. Zhou, B. Gao, Y. Jiao, Z. Deng, Y. Tang, J. Yi, C. Tian, X. Ding, and Y. Liu, "Study of first mirror exposure and protection in HL-2A tokamak," *Fusion Engineering and Design*, vol. 81, no. 23–24, pp. 2823–2826, 2006.
- [139] M. Rubel, G. De Temmerman, P. Sundelin, J. Coad, A. Widdowson, D. Hole, F. L. Guern, M. Stamp, and J. Vince, "An overview of a comprehensive First Mirror Test for ITER at JET," *Journal of Nuclear Materials*, vol. 390–391, pp. 1066–1069, 2009.
- [140] M. Rubel, D. Ivanova, J. Coad, G. De Temmerman, J. Likonen, L. Marot, A. Schmidt, and A. Widdowson, "Overview of the second stage in the comprehensive mirrors test in JET," *Physica Scripta*, vol. 2011, no. T145, p. 014070, 2011.

- [141] L. Marot, E. Meyer, M. Rubel, D. Ivanova, A. Widdowson, J. Coad, J. Likonen, A. Hakola, S. Koivuranta, and G. De Temmerman, “Performances of Rh and Mo mirrors under JET exposure,” *Journal of Nuclear Materials*, *in press*, 2012.
- [142] M. Rubel, J. Coad, G. De Temmerman, A. Hakola, D. Hole, J. Likonen, I. Uytendhouwen, and A. Widdowson, “First Mirrors Test in JET for ITER: An overview of optical performance and surface morphology,” *Nuclear Instruments and Methods in Physics Research Section A: Accelerators, Spectrometers, Detectors and Associated Equipment*, vol. 623, no. 2, pp. 818–822, 2010.
- [143] A. Litnovsky, V. Voitsenya, T. Sugie, G. De Temmerman, A. Costley, A. Donné, K. Vukolov, I. Orlovskiy, J. Brooks, J. Allain, V. Kotov, A. Semerok, P.-Y. Thro, T. Akiyama, N. Yoshida, T. Tokunaga, and K. Kawahata, “Progress in research and development of mirrors for ITER diagnostics,” *Nuclear Fusion*, vol. 49, no. 7, p. 075014, 2009.
- [144] A. Leontyev, A. Semerok, D. Farcage, P.-Y. Thro, C. Grisolia, A. Widdowson, P. Coad, and M. Rubel, “Theoretical and experimental studies on molybdenum and stainless steel mirrors cleaning by high repetition rate laser beam,” *Fusion Engineering and Design*, vol. 86, no. 9–11, pp. 1728–1731, 2011.
- [145] Y. Zhou, L. Zheng, Y. Li, L. Li, C. Li, Y. Jiao, Z. Deng, G. Zhao, H. Gao, Q. Yang, and X. Duan, “Development of carbon deposits cleaning technique for metallic mirrors in HL-2A,” *Journal of Nuclear Materials*, vol. 415, no. 1, Supplement, pp. S1206–S1209, 2011.